Do plasma composition affect the accretion and jets associated with the compact

Blackhole shadow, M87

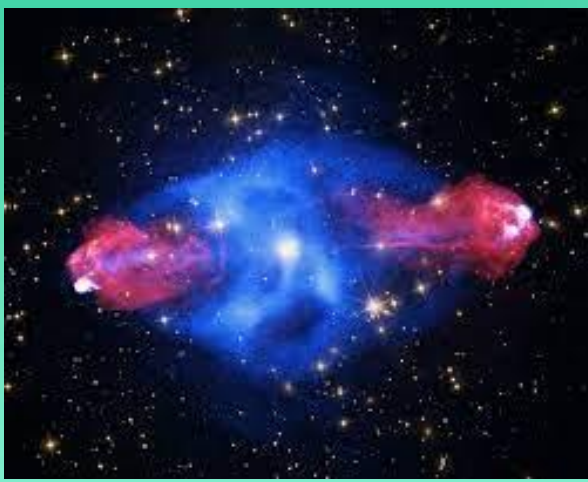

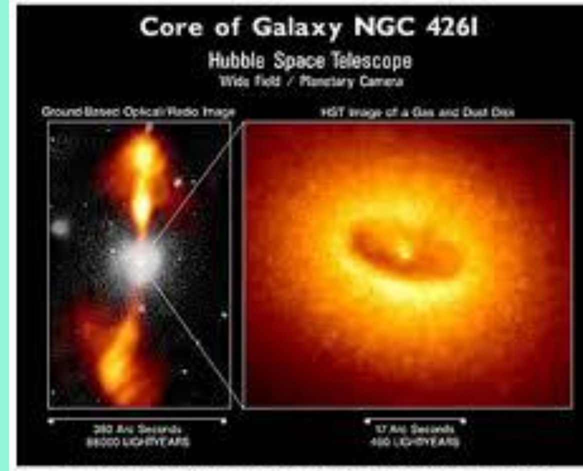

Figure 5: Active galaxy NGC 4261 at radio and optical wavelengths.

Cygnus A

AGN, NGC 4261

Indranil Chattopadhyay

Aryabhatta Research Institute of observational sciencES

indra@aries.res.in

AAPCOS 2023, SINP, 24 Jan 2023

Accretion is the best model to explain the luminosity, spectra and timing properties from AGNs and microquasars (supposed site of stellar mass BHs or NS)

(artist's impression)

Accretion is the best model to explain the luminosity, spectra and timing properties from AGNs and microquasars (supposed site of stellar mass BHs or NS)

(artist's impression)

Also jets and outflows are observed to be associated with these objects i.e., a fraction of the accreting matter are redirected as bipolar jets

M87 jet, Biretta's page

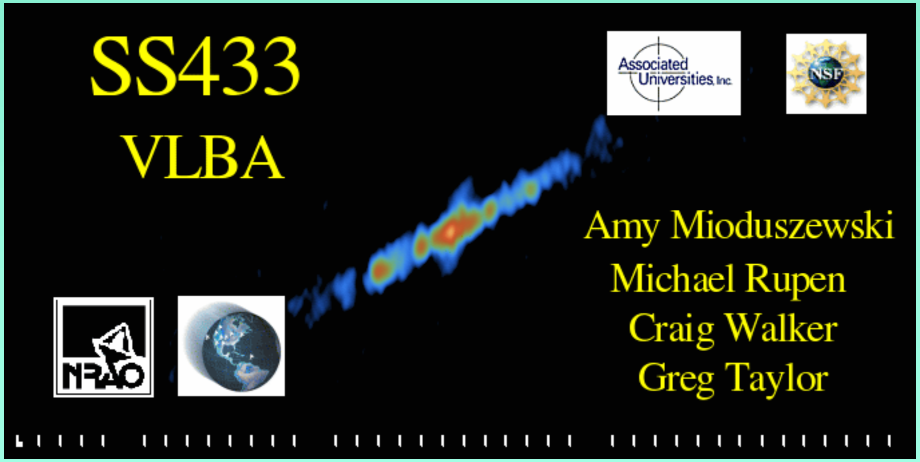

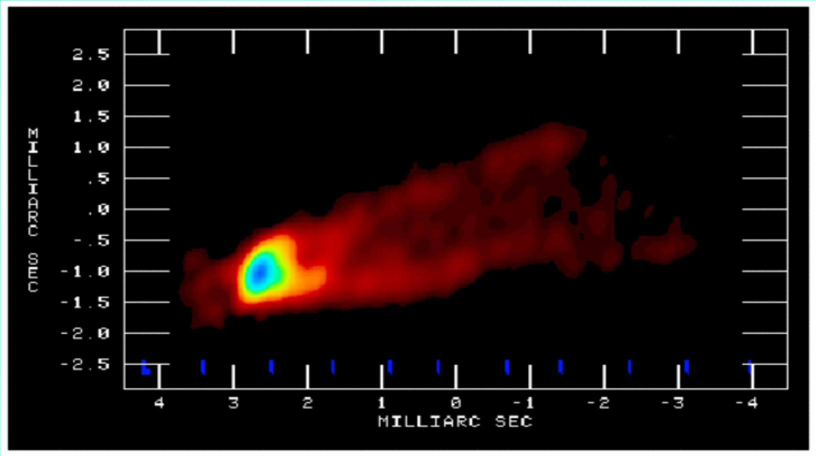

B) What has been inferred thus far:

- **Accretion onto black hole is trans-relativistic, in nature, i.e., at large distance the flow is non-relativistic but close to the horizon the flow is relativistic.**
- **The jets are thermally relativistic near the base, but relativistic speeds far away**
- **The important point to note is that, jets are launched from the accretion disc and that the matter is quite hot! ($T_e > 10^9$ K). But further out the T would be non-relativisitic.**
- **Therefore, the plasma around compact object are full ionized and thermally relativistic i.e., KT ~ mc^2**

Generally we consider the gas particles to obey Newtonian kinetic theory (Γ – constant), even if we use relativistic equations of motion, to describe the dynamics of flow around compact objects.

In other words, the particles that constitute the gas/fluid/plasma follow Maxwell-Boltzmann distribution or distribution function

$f \sim \exp(-mw^2/2kT)$; w= instantaneous random velocity

So the average energy density of these particles

$e = p/(\Gamma-1)$; for relativistic gas add rest mass

$e = \rho c^2 + p/(\Gamma-1)$

In other words, the particles that constitute the gas/fluid/plasma follow Maxwell-Boltzmann distribution or distribution function

$f \sim \exp(-mw^2/2kT)$; w= instantaneous random velocity

So the average energy density of these particles

$e = p/(\Gamma-1)$; for relativistic gas add rest mass

$e = \rho c^2 + p/(\Gamma-1)$ [Closure relation or Equation of state]

The problem is there is no information of composition!

In other words, the particles that constitute the gas/fluid/plasma follow Maxwell-Boltzmann distribution or distribution function

$f \sim \exp(-mw^2/2kT)$; w= instantaneous random velocity

So the average energy density of these particles

$e = p/(\Gamma-1)$; for relativistic gas add rest mass

$e = \rho c^2 + p/(\Gamma-1)$ [Closure relation or Equation of state]

The problem is there is no information of composition!

A consistent relativistic EoS can be computed from first principles. Considering energy of each gas particles as

$$\varepsilon = \sqrt{m^2c^4 + q^2c^2}$$ llowing a distribution $$P_s \propto \exp\left(-\frac{\varepsilon}{kT}\right)$$

Gives the energy density

$$e_C = \rho c^2 \frac{3K_3(1/\Theta) + K_1(1/\Theta)}{4K_2(1/\Theta)}$$

$$h = \frac{e+p}{\rho c^2} = \frac{K_3(\rho c^2/p)}{K_2(\rho c^2/p)}$$

This is the famous Chandrashekhar EoS and is being abbreviated as RP (relativistic perfect)! Where, K2 & K3 are modified Bessels function of the 2nd & 3rd kind. (Chandrashekhar 1938, Synge 1957, Cox&Giuli 1968)

The problem with RP EoS is that,

- it is expensive to implement in numerical simulation codes.

The problem with RP EoS is that,

- it is expensive to implement in numerical simulation codes.

- We used an algebraic relativistic EoS a close approximate of RP to implement in numerical codes.
- We extended it from single species to multiple species ionized fluid.
- The EoS is:

$$e = n_{e^-} m_e c^2 f$$

[CR EoS]

$$f = (2-\xi)\left[1+\Theta\left(\frac{9\Theta+3}{3\Theta+2}\right)\right] + \xi\left[\frac{1}{\eta}+\Theta\left(\frac{9\Theta+3/\eta}{3\Theta+2/\eta}\right)\right]$$

$$\Theta = kT/(m_e c^2)$$

$$N = \frac{1}{2}\frac{\mathrm{d}f}{\mathrm{d}\Theta};\ \ \Gamma = 1 + \frac{1}{N}$$

(polytropic index)

The problem with RP EoS is that,

- it is expensive to implement in numerical simulation codes.

- We used an algebraic relativistic EoS a close approximate of RP to implement in numerical codes.
- We extended it from single species to multiple species ionized fluid.
- The EoS is:

$$e = n_{e^-} m_e c^2 f$$

[CR EoS]

$$f = (2-\xi)\left[1 + \Theta\left(\frac{9\Theta+3}{3\Theta+2}\right)\right] + \xi\left[\frac{1}{\eta} + \Theta\left(\frac{9\Theta+3/\eta}{3\Theta+2/\eta}\right)\right]$$

$$\Theta = kT/(m_e c^2)$$

$$N = \frac{1}{2}\frac{\mathrm{d}f}{\mathrm{d}\Theta}; \;\; \Gamma = 1 + \frac{1}{N}$$

(polytropic & adiabatic indices)

We use relativistic EoS proposed by Chattopadhyay & Ryu (ApJ, 2009). Which makes the adiabatic index, temperature and composition dependent.

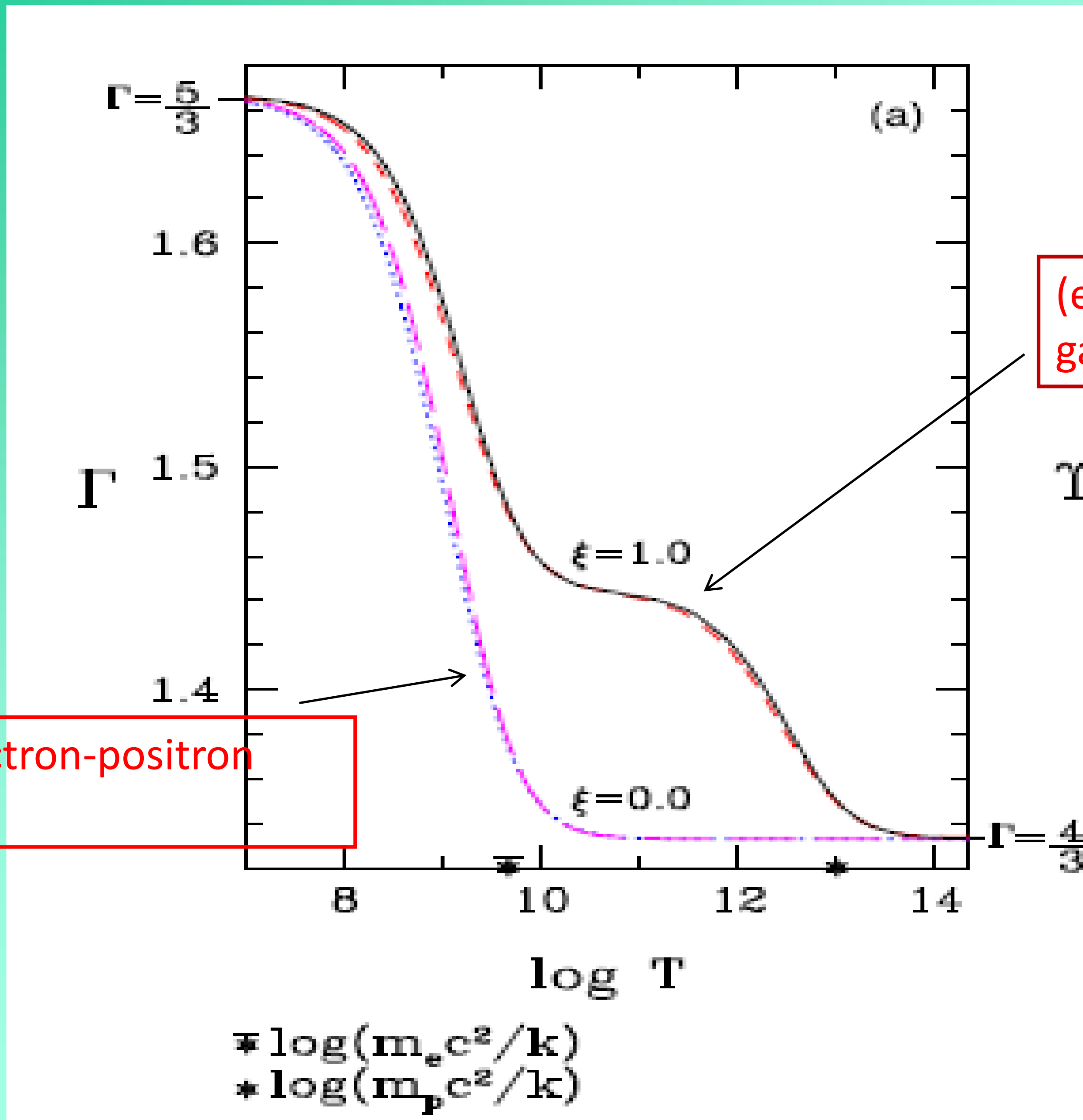

(electron-proton gas)

(electron-positron gas)

The solid & the long dashed are RP; dashed & dotted are CR

The equations of motion in most general case are

;

$$T^{\mu\nu}_{;\nu} = 0 \qquad (nu^{\nu})_{;\nu} = 0.$$

$$T^{\mu\nu} = T^{\mu\nu}_{\mathrm{M}} + T^{\mu\nu}_{\mathrm{R}} + T^{\mu\nu}_{\mathrm{EM}};$$

matter

radiation

Electro-magnetic

$$T^{\mu\nu}_{\mathrm{M}} = (e+p)u^{\mu}u^{\nu} + pg^{\mu\nu}.$$

$$T^{\mu\nu}_{\mathrm{R}} = \int I l^{\mu} l^{\nu} d\Omega.$$

$$T^{\mu\nu}_{\mathrm{EM}} = F^{\mu}_{\sigma} F^{\nu\sigma} - \frac{g^{\mu\nu} F^{\lambda\sigma} F_{\lambda\sigma}}{4}$$

Black hole accretion

Momentum balance equation is $$(g^i_\alpha + u^i u_\alpha) T^{\alpha\beta}_{;\beta} = 0$$

First law of thermodynamics is $$u_\alpha T^{\alpha\beta}_{;\beta} = 0$$

Integrating the above equations we obtain the generalized, relativistic Bernoulli parameter… a constant of motion, even in presence of dissipation. In Kerr metric it is

$$E = h\gamma_v \exp X_f$$

$$X_{f1} = \int \left[\frac{1 - a_s^2/r^2}{r^2(1 - 2/r + a_s^2/r^2)} + \frac{l^2}{2r^3 \mathscr{D} \gamma_v^2} - \frac{(0.5r^3 \mathscr{A} + r^3 - a_s^2)(l^2/\mathscr{A} + \omega\gamma\sqrt{\frac{\mathscr{A}}{\mathscr{D}}})}{r^2 \gamma_v^2} \right] dr$$

$$X_{f2} = \int \left[\frac{g^{\phi\phi} g_{rr} \tilde{\tau} \rho u^r (L - L_0)^2}{2\eta(f + 2\Theta)} - \frac{\Lambda}{(e+p) u^r g^{rr} \gamma_v^2} - \frac{S^r}{(e+p)\mathscr{D}} \right] dr$$

$X_f = X_{f1} + X_{f2}$, $\quad S^r = u^r t_{\phi r} \sigma^{r\phi}$

In absence of dissipation $\quad \gamma_v \exp X_f = -u_t$

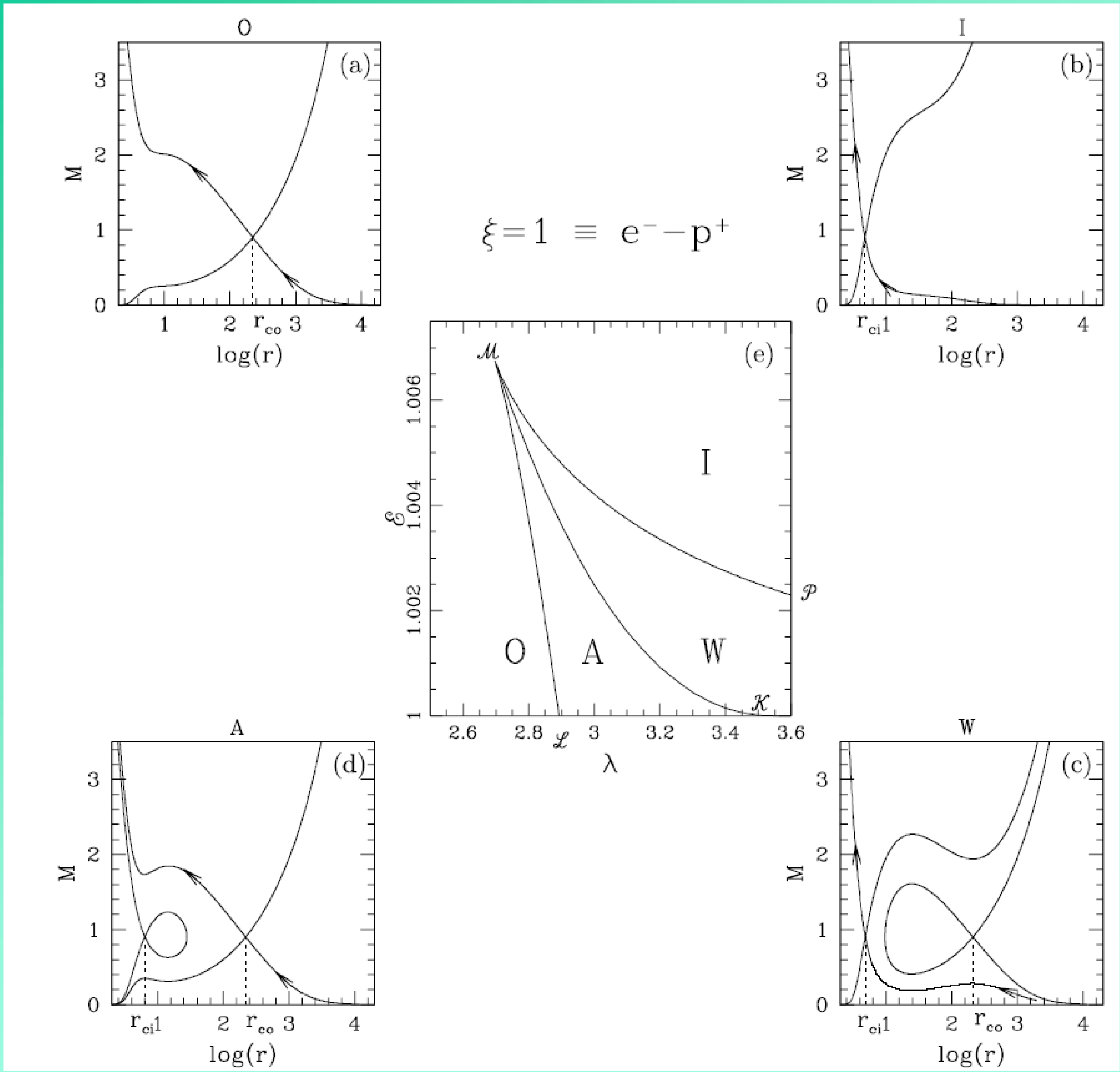

As angular momentum is varied; different solutions are obtained. The flow solutions are transonic. This is a typical GR or strong gravity effect.

Multiple sonic points are due to the interplay of gravity and rotation

Fig. 2. The domain for multiple-critical points in $\mathcal{E}-\lambda$ space, is the MCP region (e). $M - \log(r_c)$ plot of the O type (a); I type (b); W type (c); and A type (d). Solutions are presented. The solution type are also marked above each figure. The arrows mark the smooth global accretion solutions. All the figures are for $e^- - p^+$ flow ($\xi = 1.0$). The dotted vertical lines mark the positions of physical critical points.

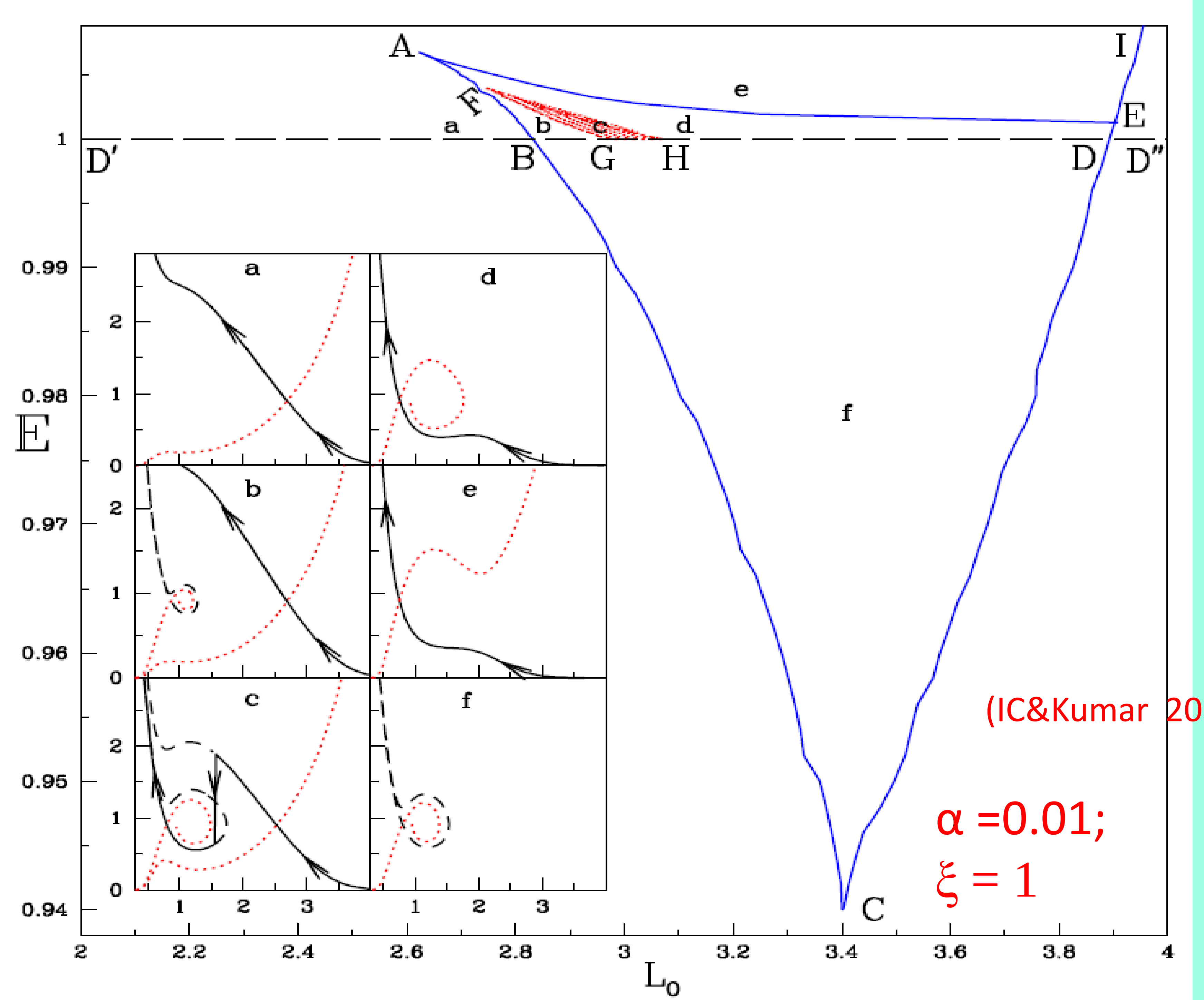

A
I
e
F
E
a
b
c
d
1
D′
B
G
H
D
D″
0.99
0.98
0.97
0.96
0.95
0.94
𝔼
f
2
3.4
L_0
C
(IC&Kumar 2016)
α =0.01;
ξ = 1

Effect of composition in accretion

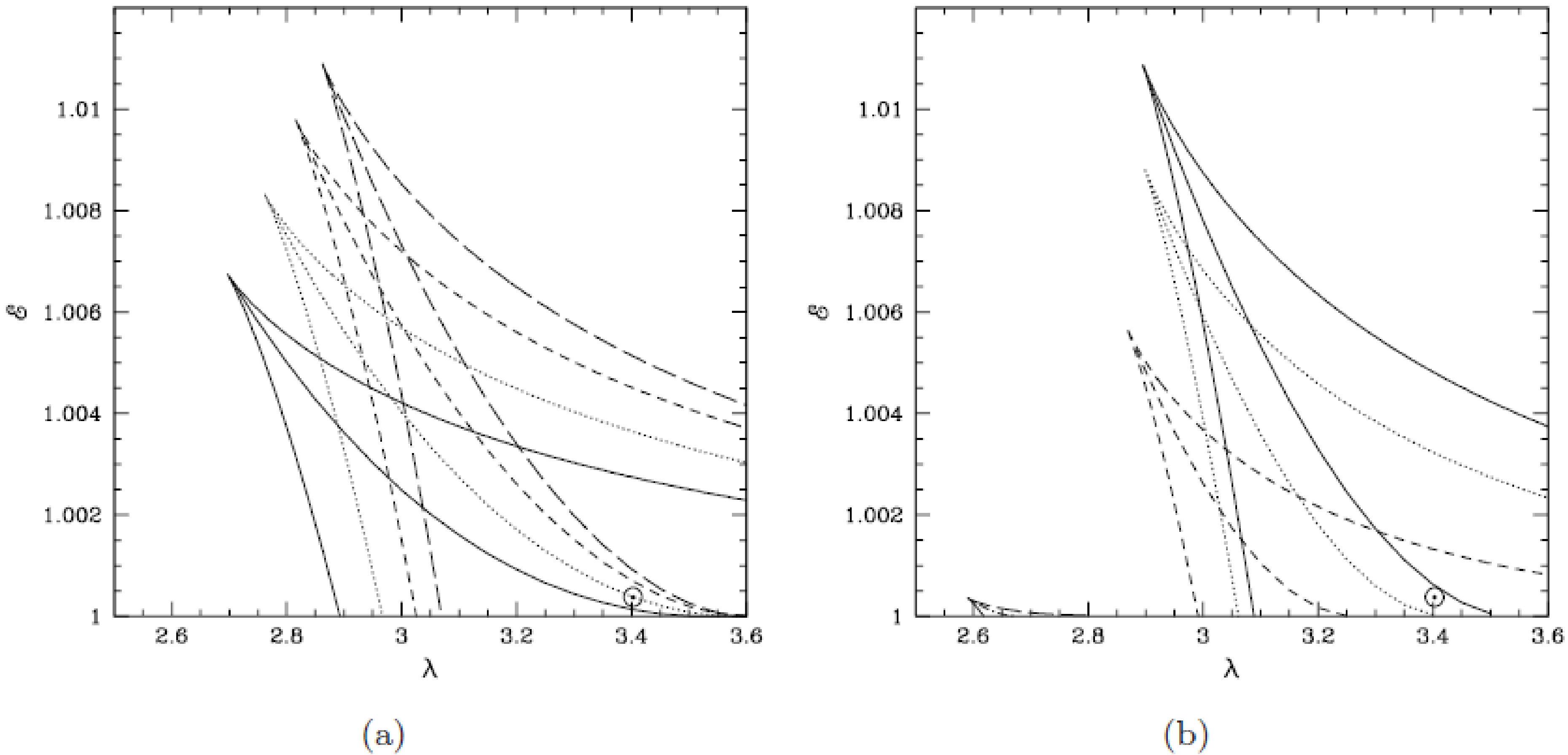

Fig. 5. (a) The $\mathcal{E}-\lambda$ parameter space for multiple critical point (the MCP region) for $\xi = 1$ (solid), 0.8 (dotted), 0.6 (dashed) and 0.4 (long dashed). (b) The MCP region for $\xi = 0.2$ (solid), 0.1 (dotted), 0.05 (dashed) and 0.01 (long dashed). The circled-dot is located at $\mathcal{E} = 1.0004$ and $\lambda = 3.4$ of the parameter space. $\mathcal{LMP}$ is not explicitly written to avoid clumsiness.

Effect of composition in accretion

Flows with protons may harbour multiple sonic points, BUT electron-positron pair plasma can harbor **only one sonic point**!

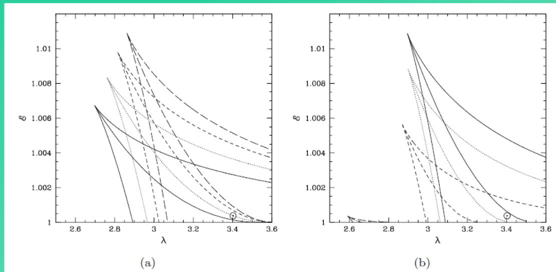

Fig. 5. (a) The $\mathcal{E}-\lambda$ parameter space for multiple critical point (the MCP region) for $\xi = 1$ (solid), 0.8 (dotted), 0.6 (dashed) and 0.4 (long dashed). (b) The MCP region for $\xi = 0.2$ (solid), 0.1 (dotted), 0.05 (dashed) and 0.01 (long dashed). The circled-dot is located at $\mathcal{E} = 1.0004$ and $\lambda = 3.4$ of the parameter space. $\mathcal{LMP}$ is not explicitly written to avoid clumsiness.

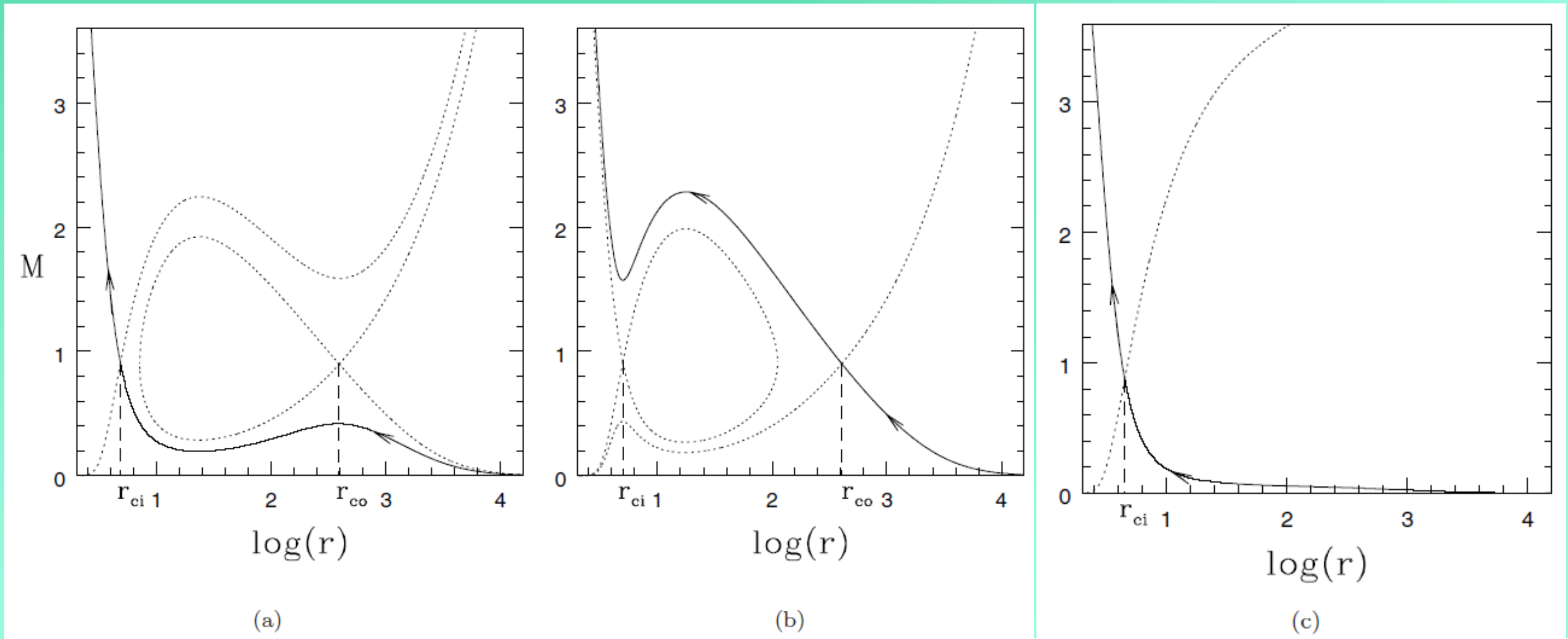

Fig. 6. The Mach number M is plotted with $\log(r)$ for $\{\mathcal{E}, \lambda\} = \{1.0004, 3.4\}$. (a) $e^- - p^+$ flow i.e. $\xi = 1.0$, the dotted curve through r_{ci} is the wind type solution and the α type solution is through r_{co}. (b) A flow with $\xi = 0.5$, the dotted curve through r_{co} is the wind type solution and the reflected-α type solution is through r_{ci}. (c) $e^- - e^+$ flow i.e. $\xi = 0.0$ and the dotted curve through r_{ci} is a wind type solution. In all the figures, the solid curve with arrows, are the smooth global accretion solutions.

Accretion one-dimensional result:

Use Paczynsky-Wiita potential

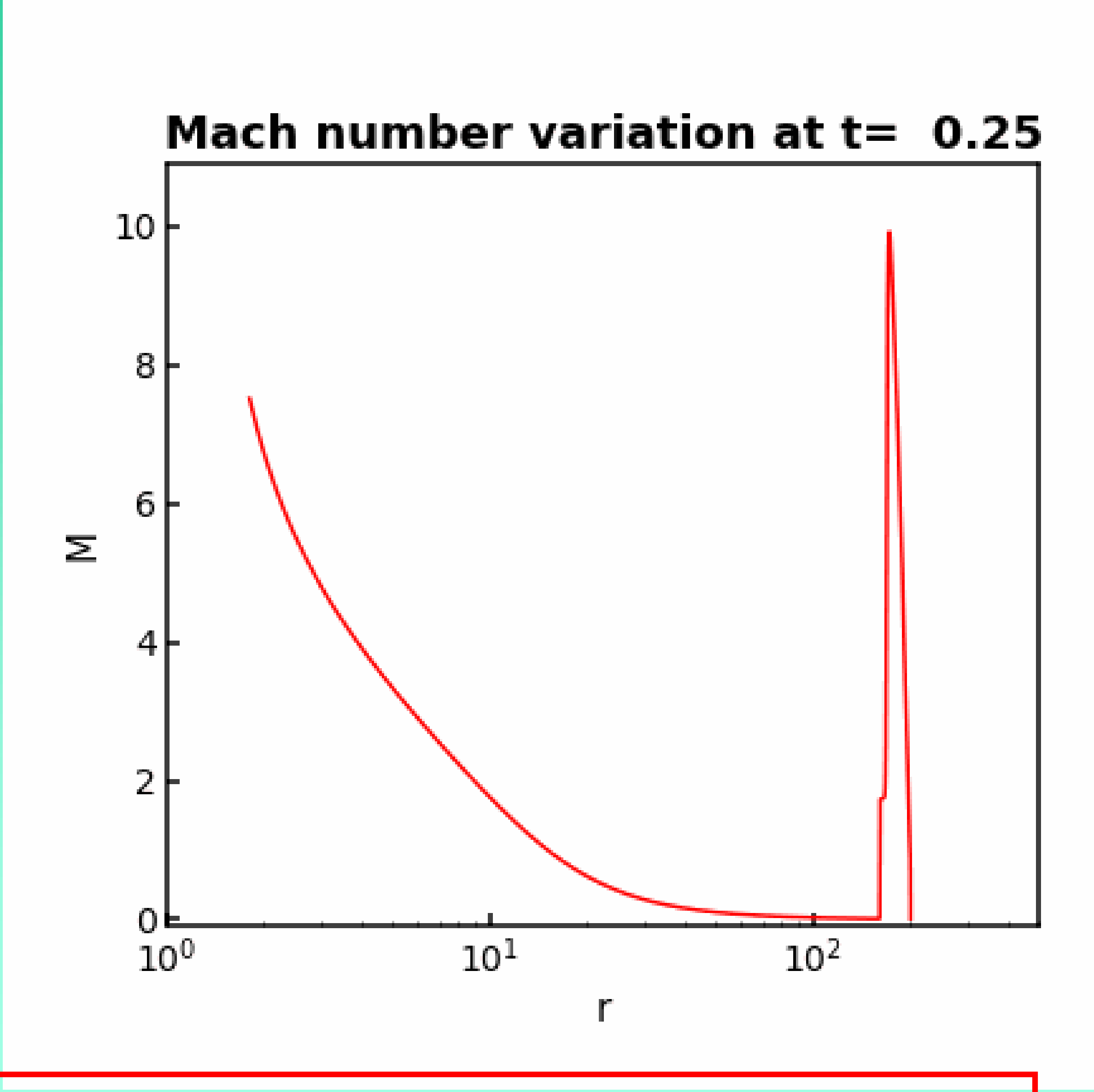

Smooth accretion solution, along equatorial plane

Composition $\xi = 1$; electron-proton flow

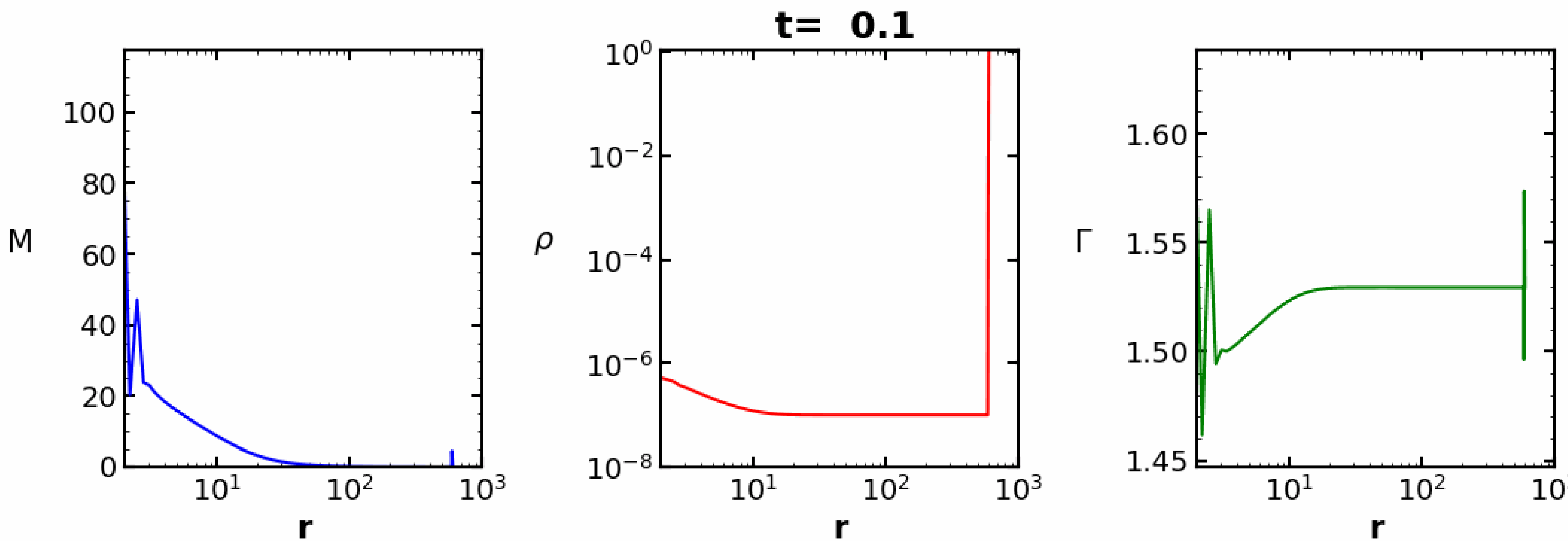
t= 0.1
M
100
80
60
40
20
0
ρ
10^{0}
10^{-2}
10^{-4}
10^{-6}
10^{-8}
Γ
1.60
1.55
1.50
1.45
10^{1}
10^{2}
10^{3}
r

E=1.0002; λ=1.75

Comparison with analytical solution

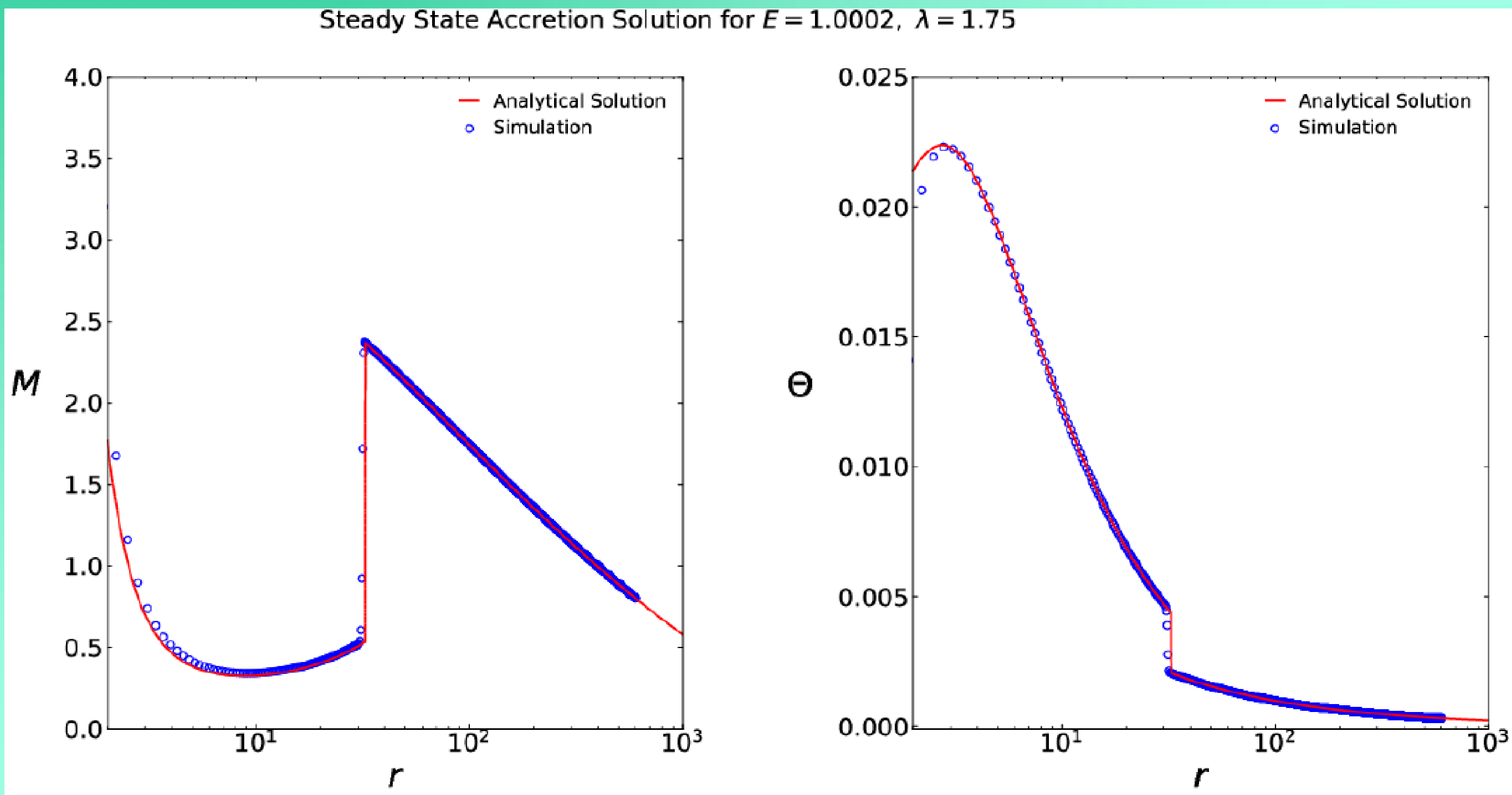

However, for the same injection parameters if the composition is changed to ξ=0.25, the shock goes away!

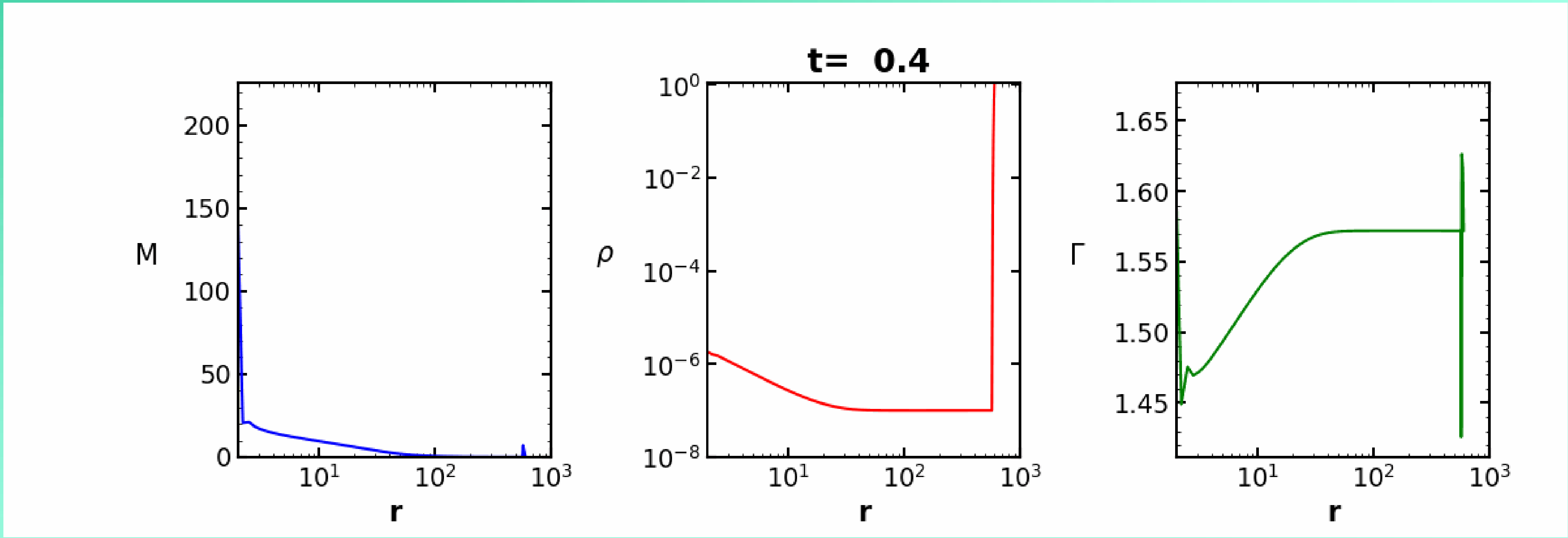

vinj= 1.77e-02; Θinj = 3.199e-03 ; λinj = 1.75

Now if for electron-proton flow the velocity (11%) and temperature (9%) is changed

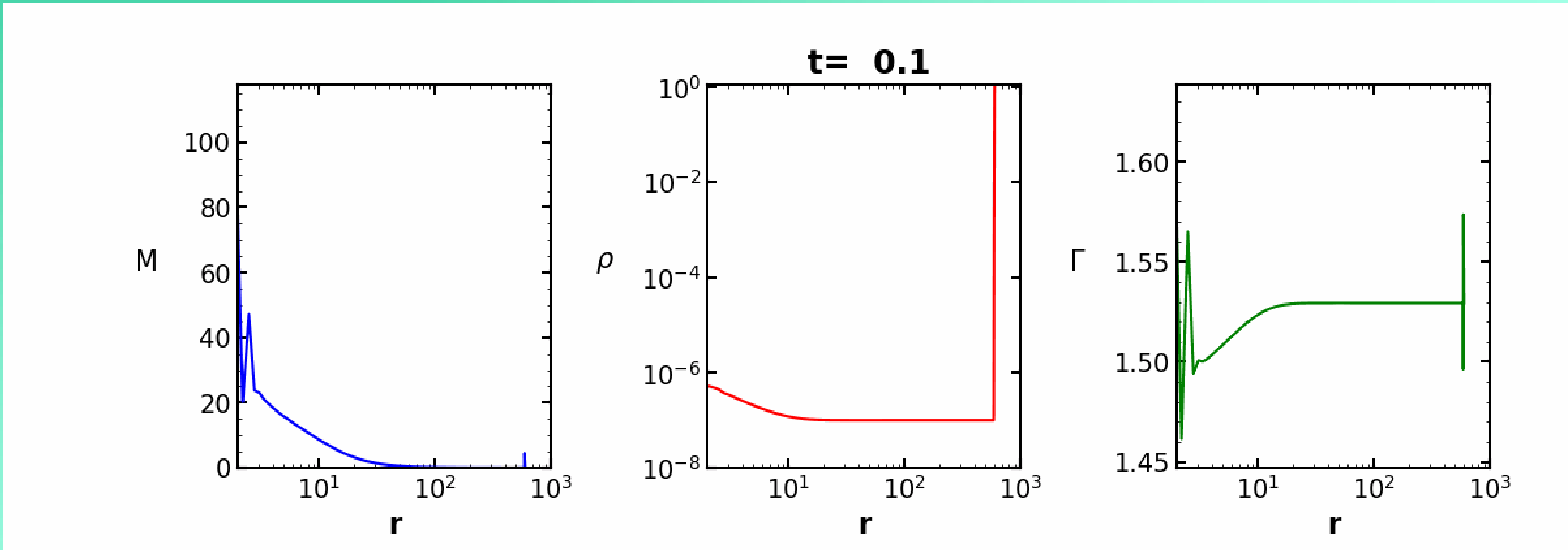

However if one check solutions with the same injection parameters including viscosity parameter

$\xi = 1.0$

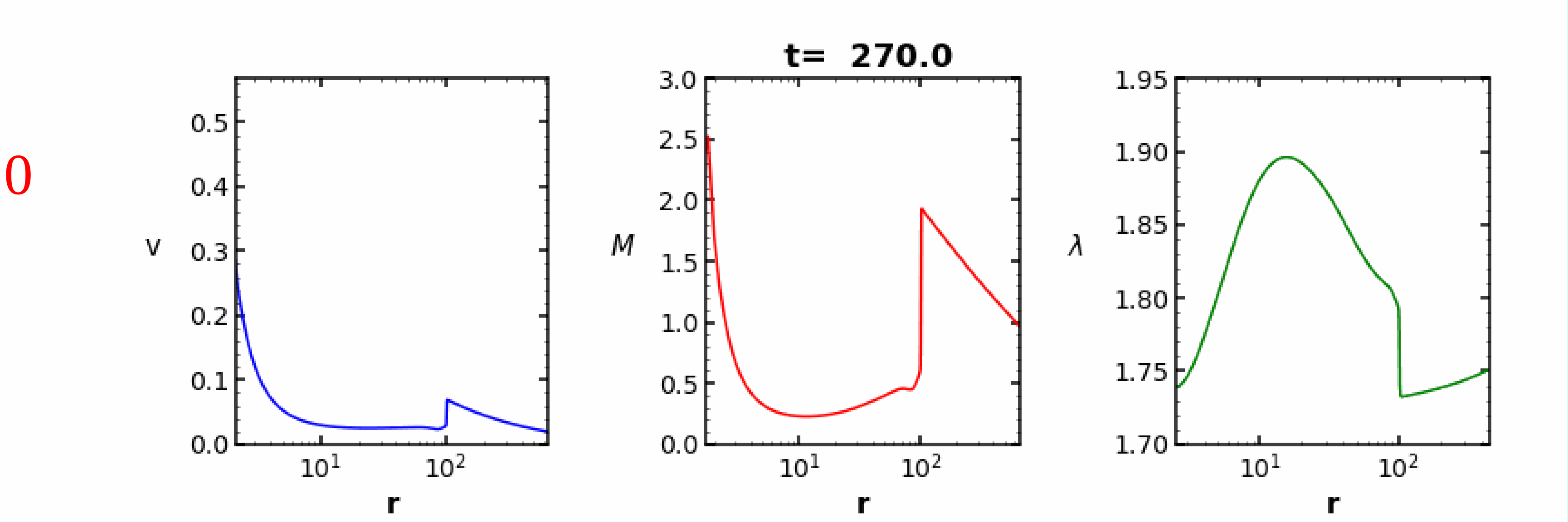

However if one check solutions with the same injection parameters including viscosity parameter

$\xi = 1.0$

$\xi = 0.8$

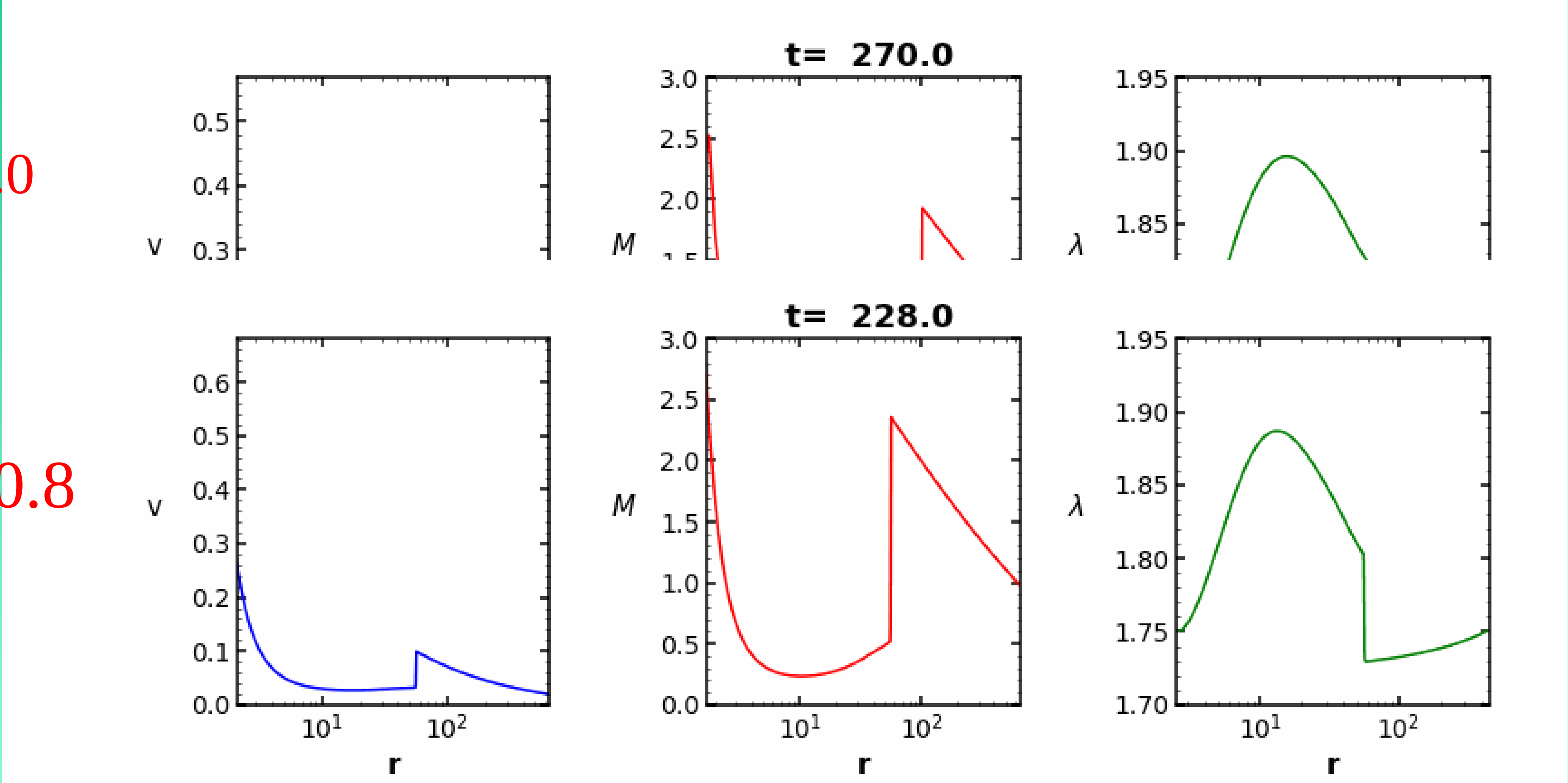

$\xi = 1.0$

$\xi = 0.8$

$\xi = 0.5$

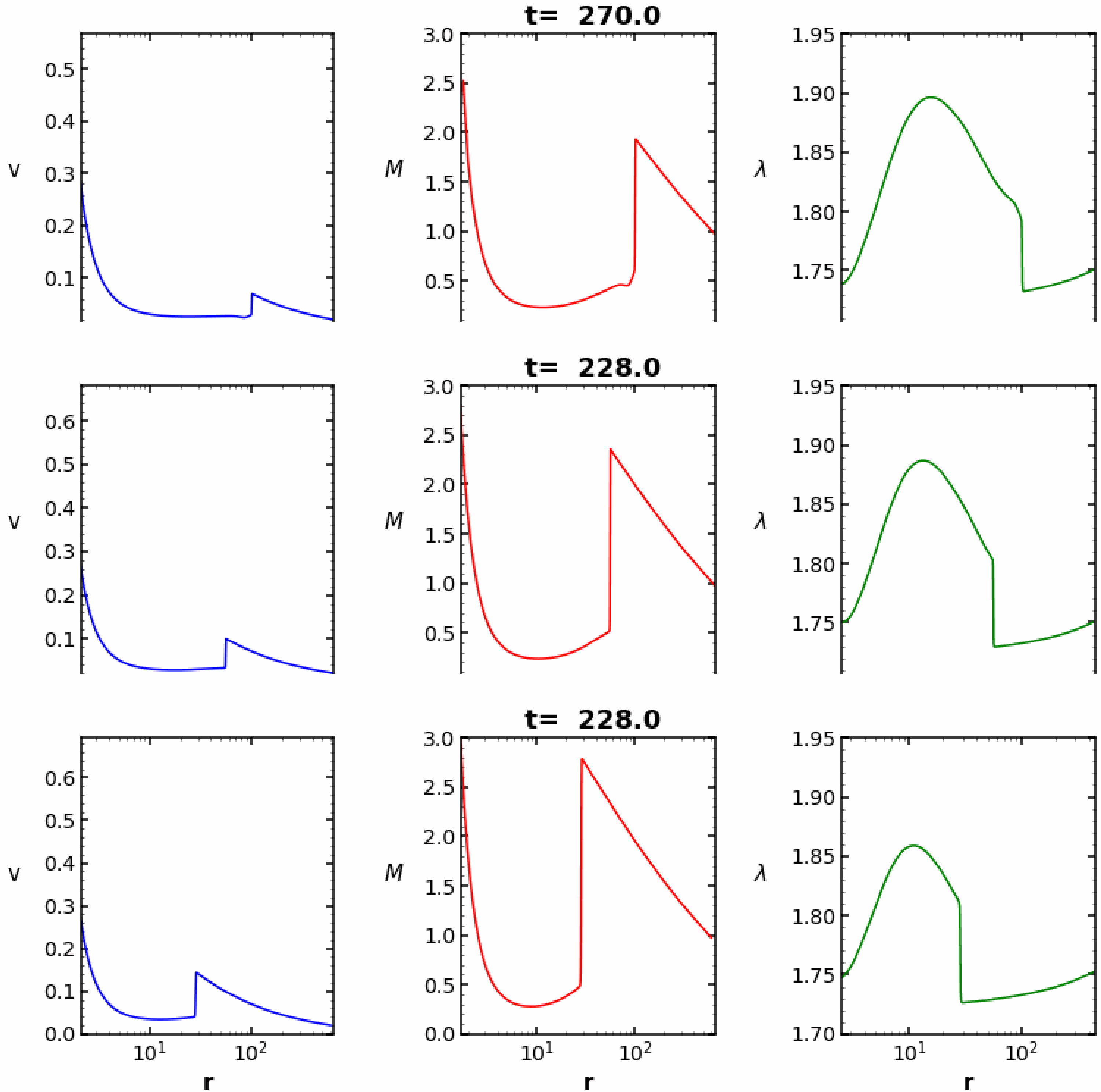

Comparing the timing property of the solution

ξ=1.0

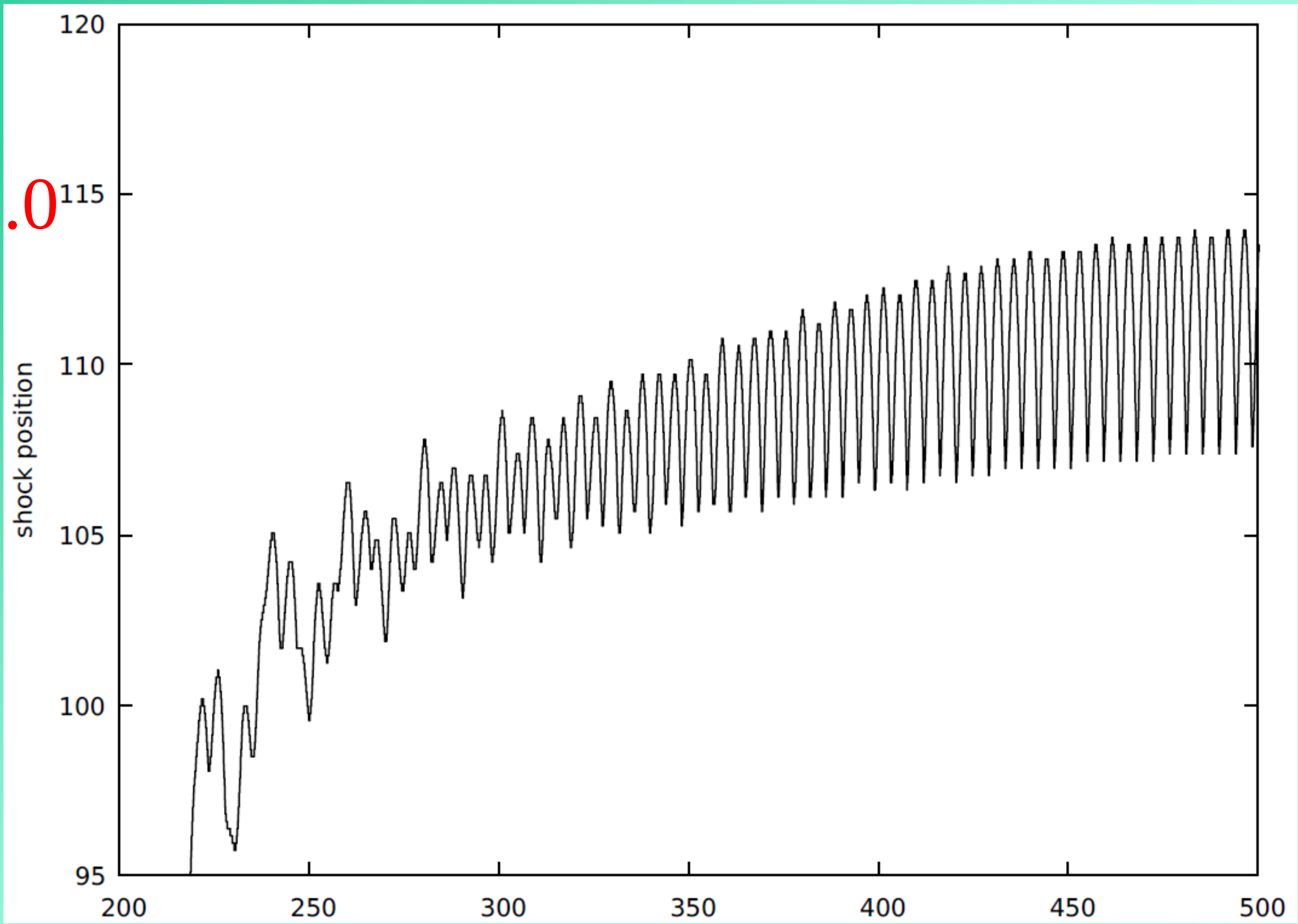

Comparing the timing property of the solution

ξ=1.0

ξ=0.8

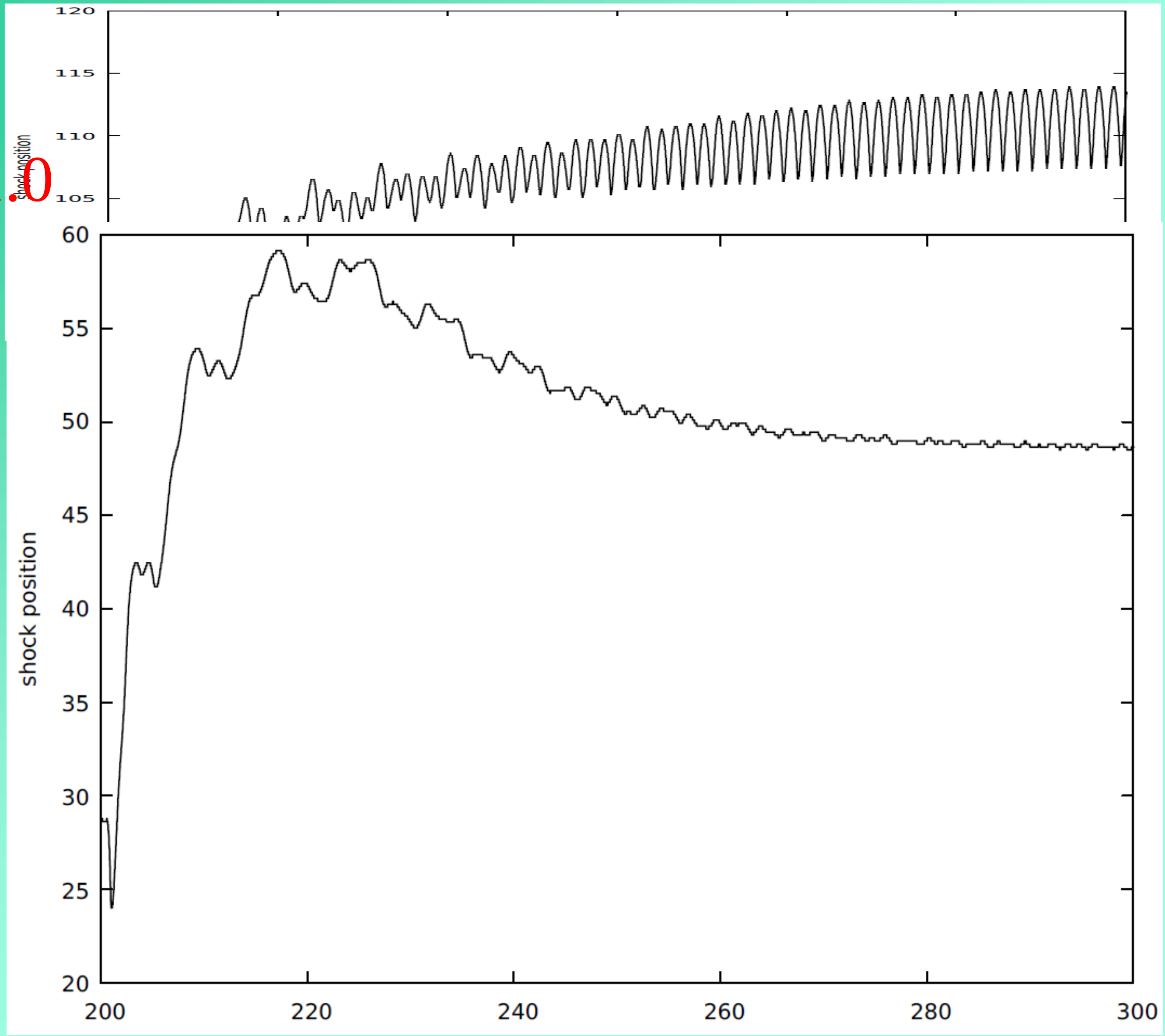

Comparing the timing property of the solution

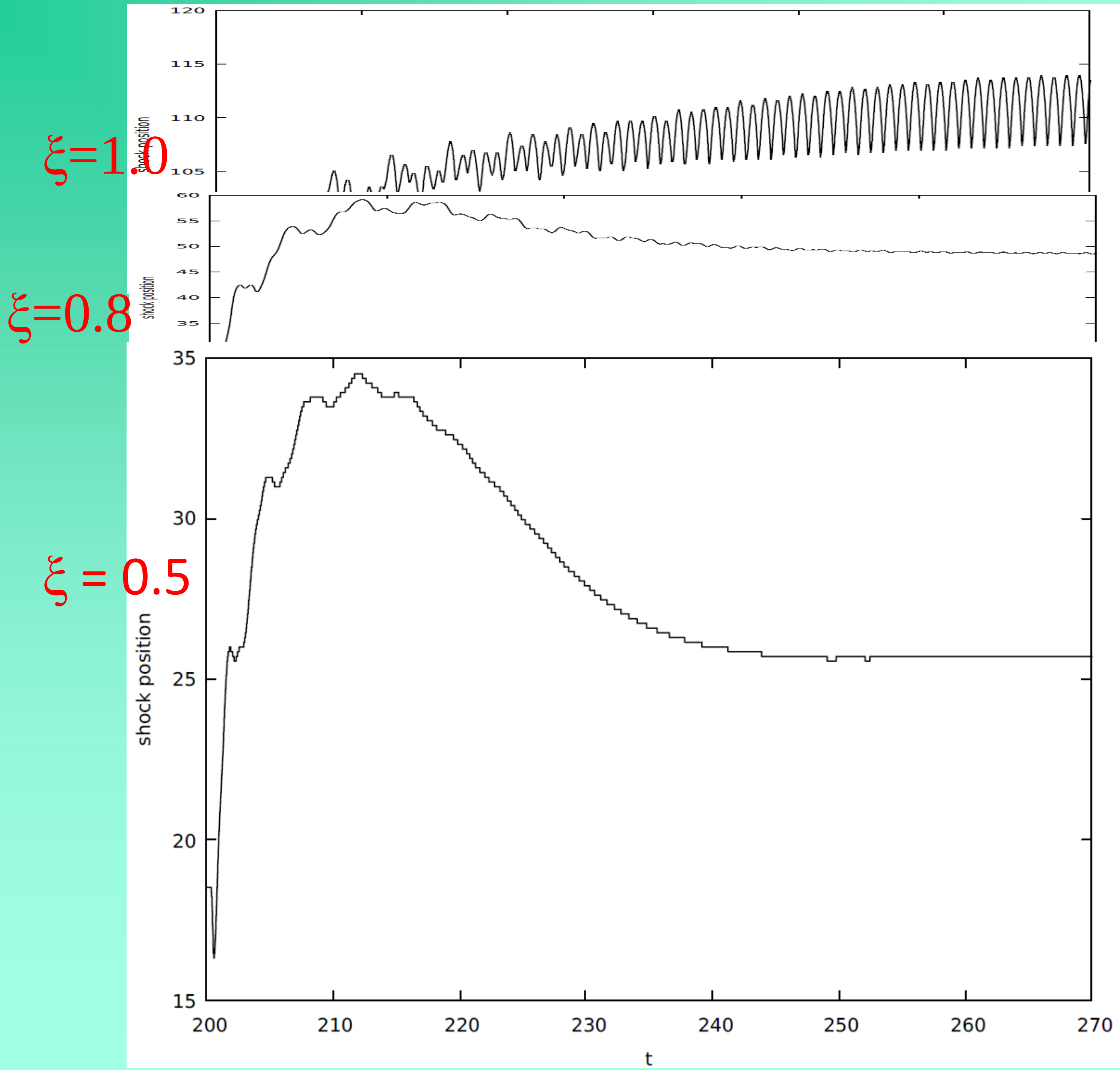

Thick disc configurations

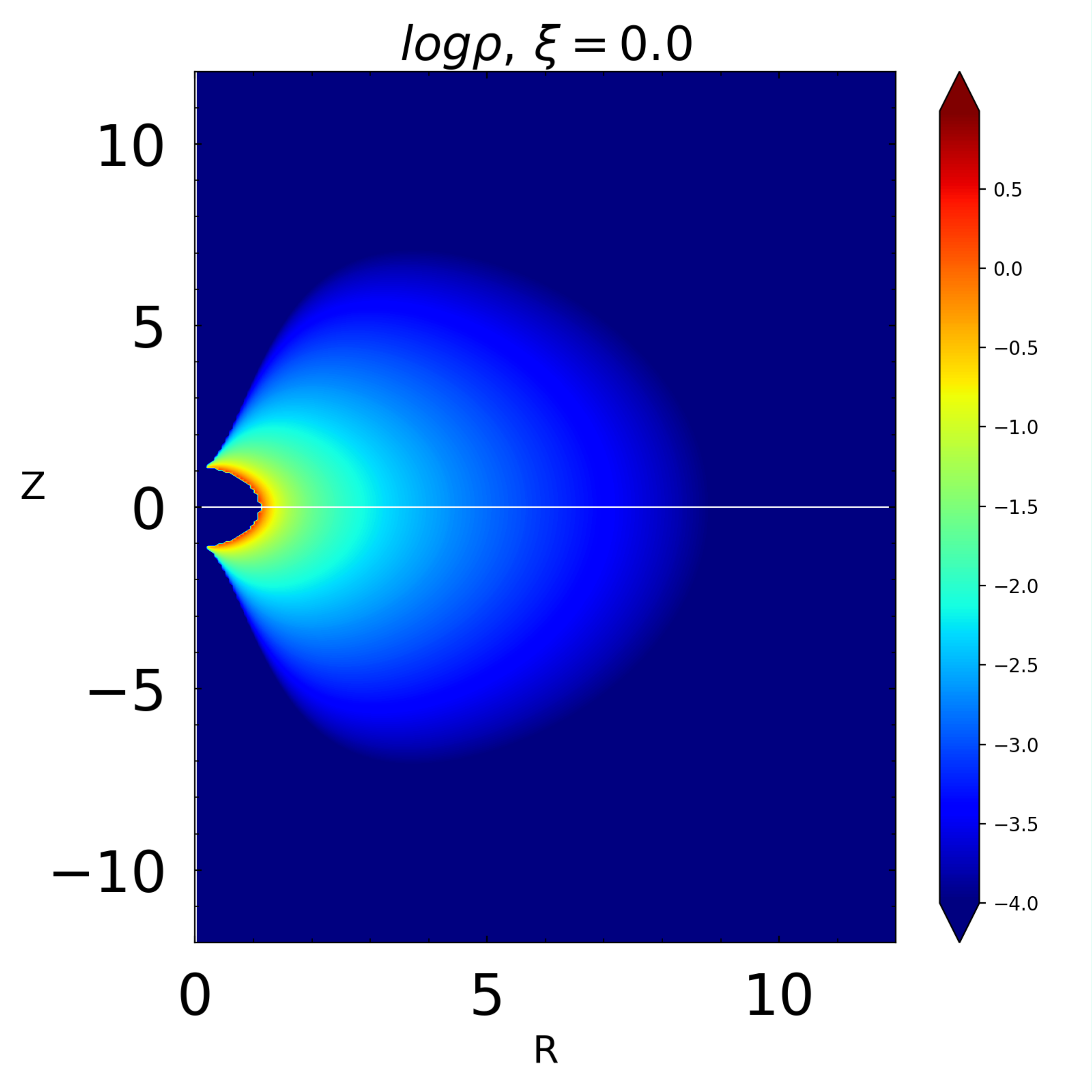

Thick disc configurations

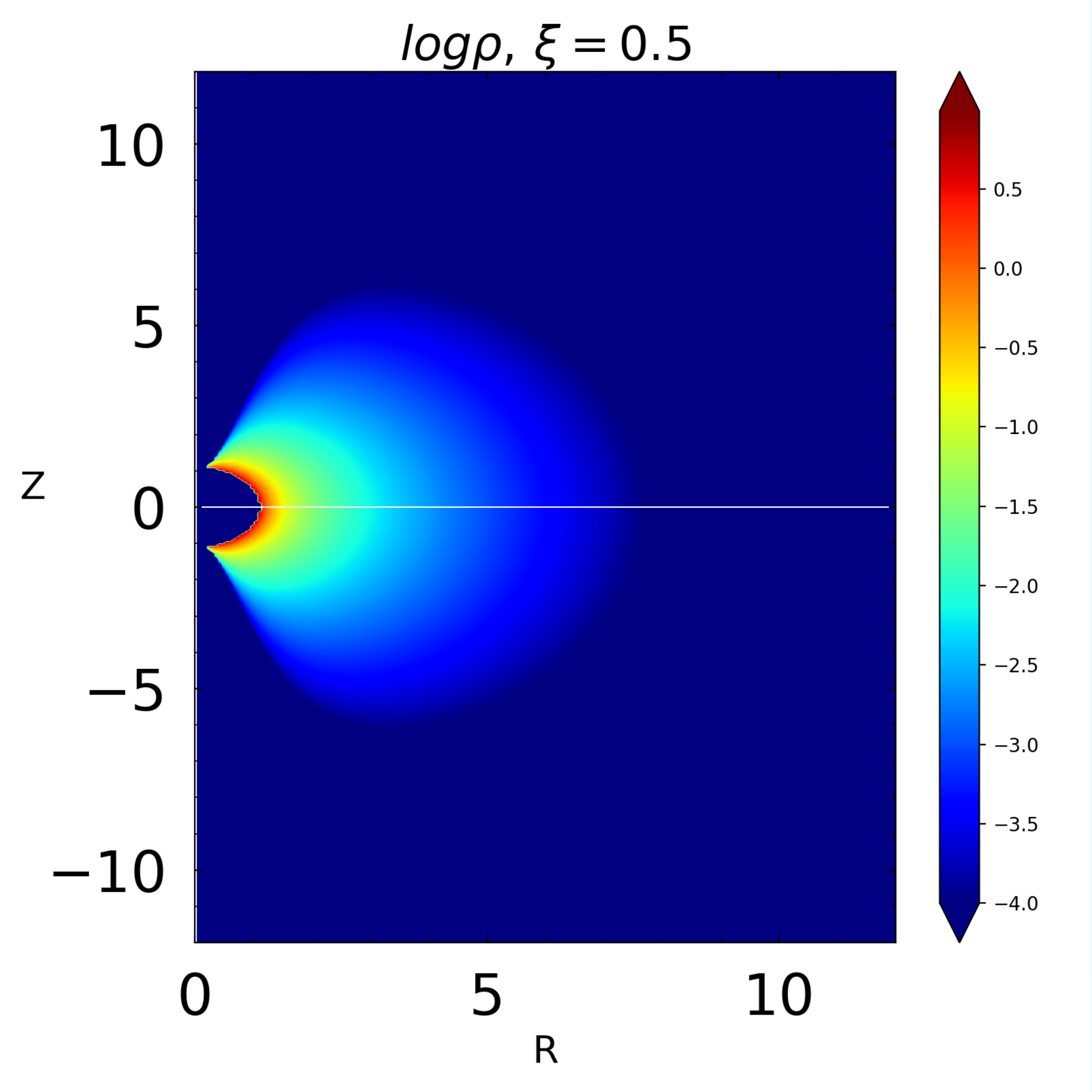

Thick disc configurations

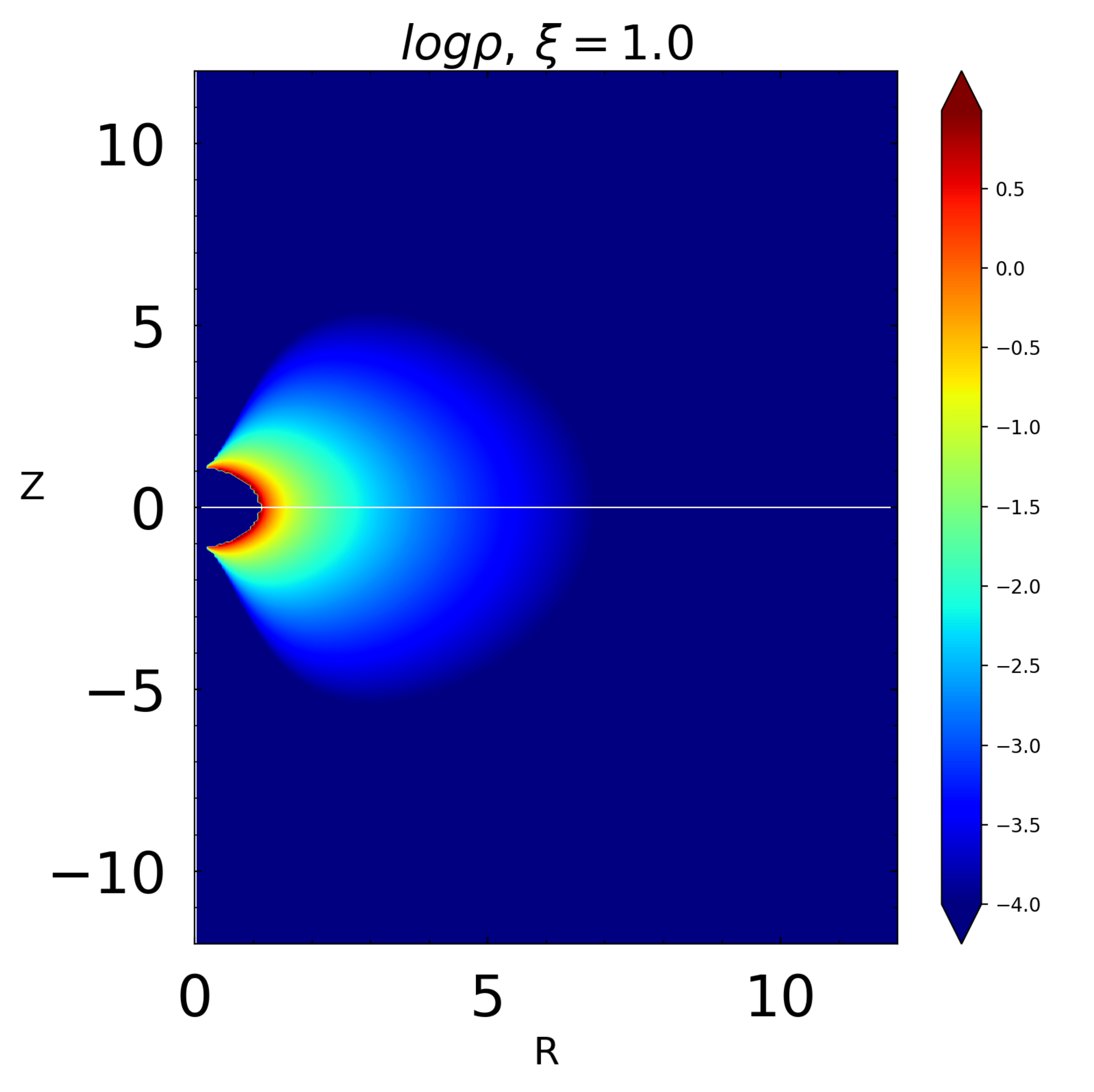

Neutron Star accretion

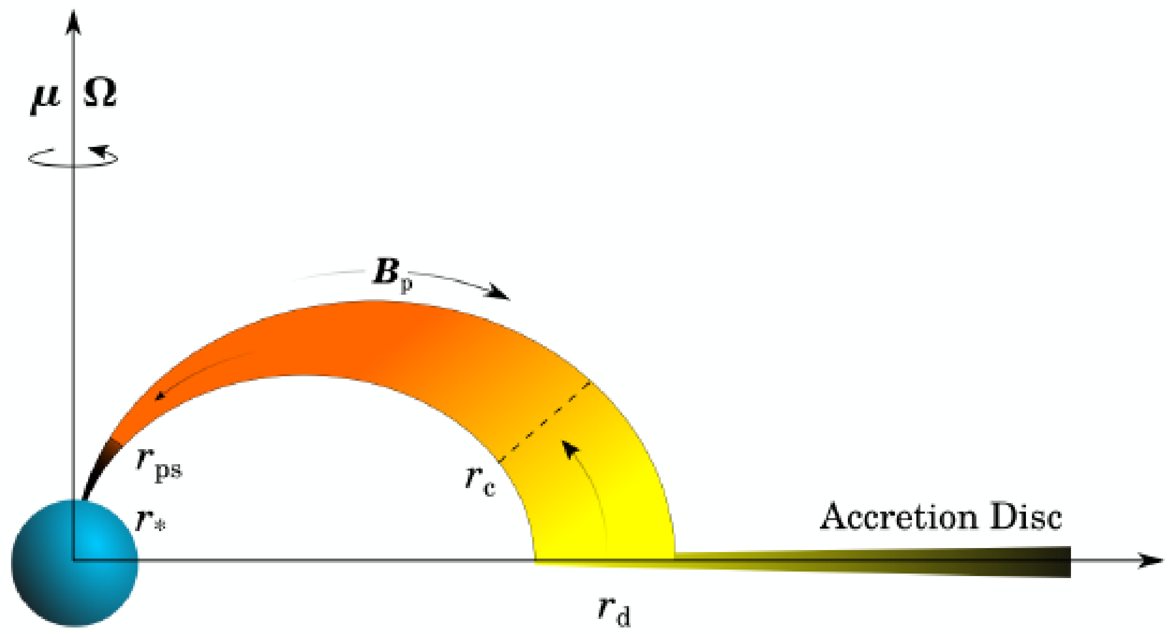

Figure 1. Representation of a magnetized accretion flow. The disk radius is marked as r_d, sonic point as r_c, primary shock as r_{ps} and r_* is the radius of the star.

Neutron Star accretion

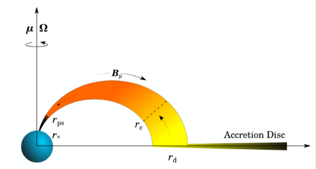

Figure 1. Representation of a magnetized accretion flow. The disk radius is marked as r_d, sonic point as r_c, primary shock as r_{ps} and r_* is the radius of the star.

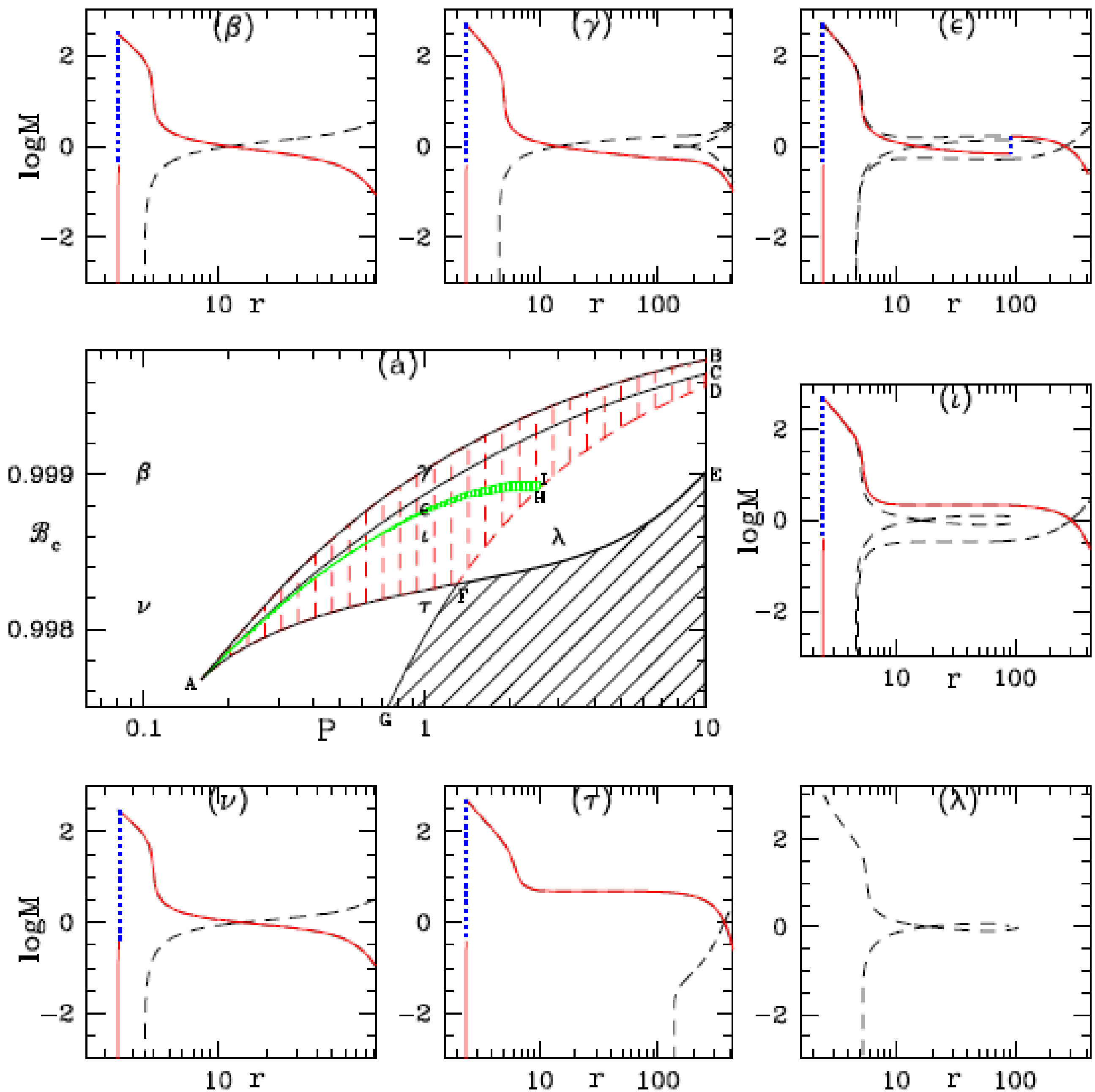

Probably for the first time, we showed a zoo of NS accretion solutions and a how the accretion depends on specific energy and spin period

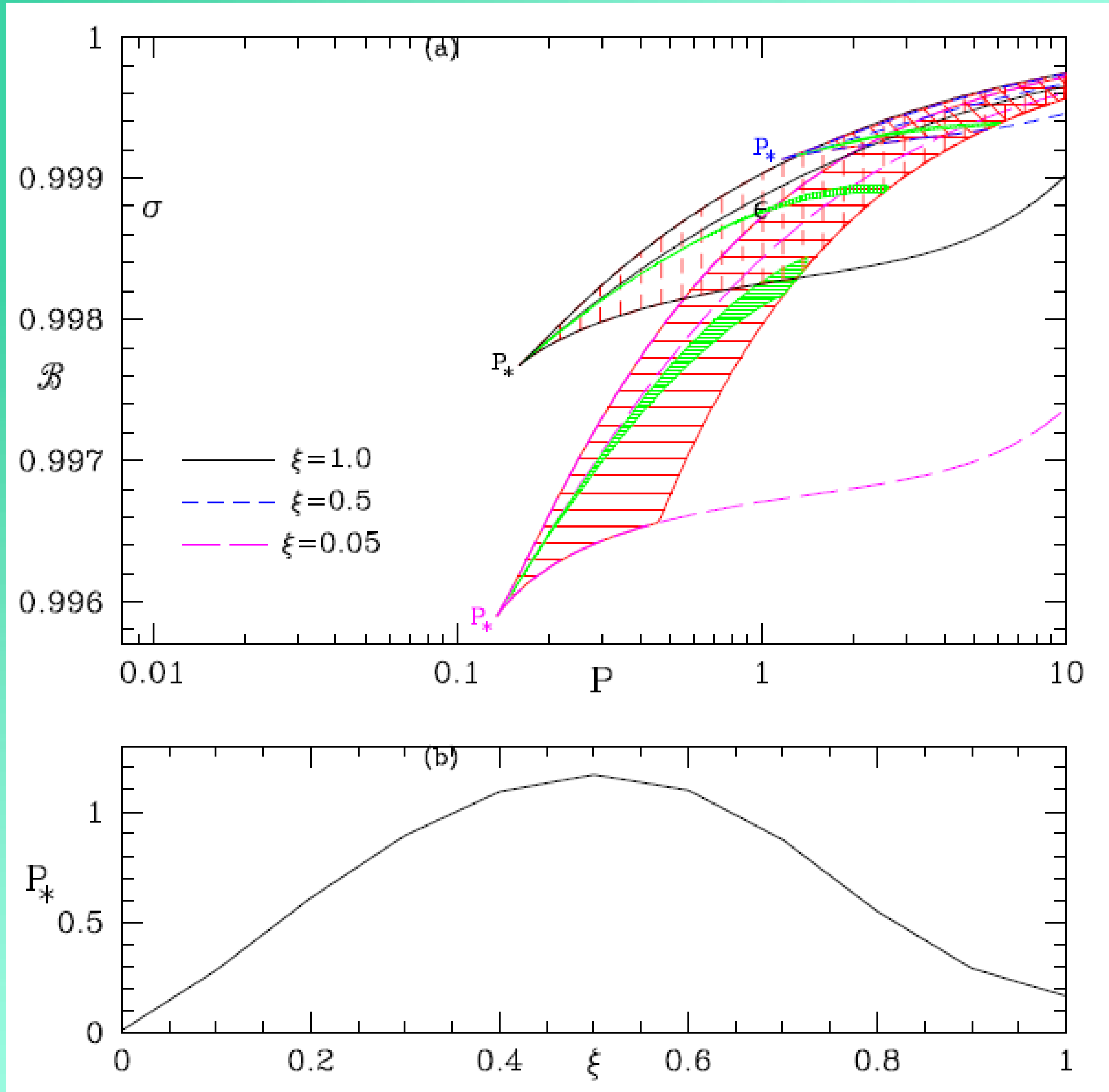

Figure 9. (a) $\mathcal{B}$–P parameter space, in which MCP region is demarcated for $\xi = 0.05$ (long-dashed, magenta), $\xi = 0.5$ (dashed, blue), and $\xi = 1.0$ (solid, black). P_* is the minimum P beyond which MCP is possible. Two coordinate points are marked as 'σ' and ϵ', the values of $\mathcal{B}$, P corresponding to these points are used to obtain accretion solutions in Figs 10 and 11, respectively. (b) P_* plotted as a function of ξ. Here, $\dot{M}_{0.01s} = 0.35 \times 10^{14}\ \mathrm{g\,s^{-1}} - \dot{M}_{10.0s} = 3.5 \times 10^{16}\ \mathrm{g\,s^{-1}}$.

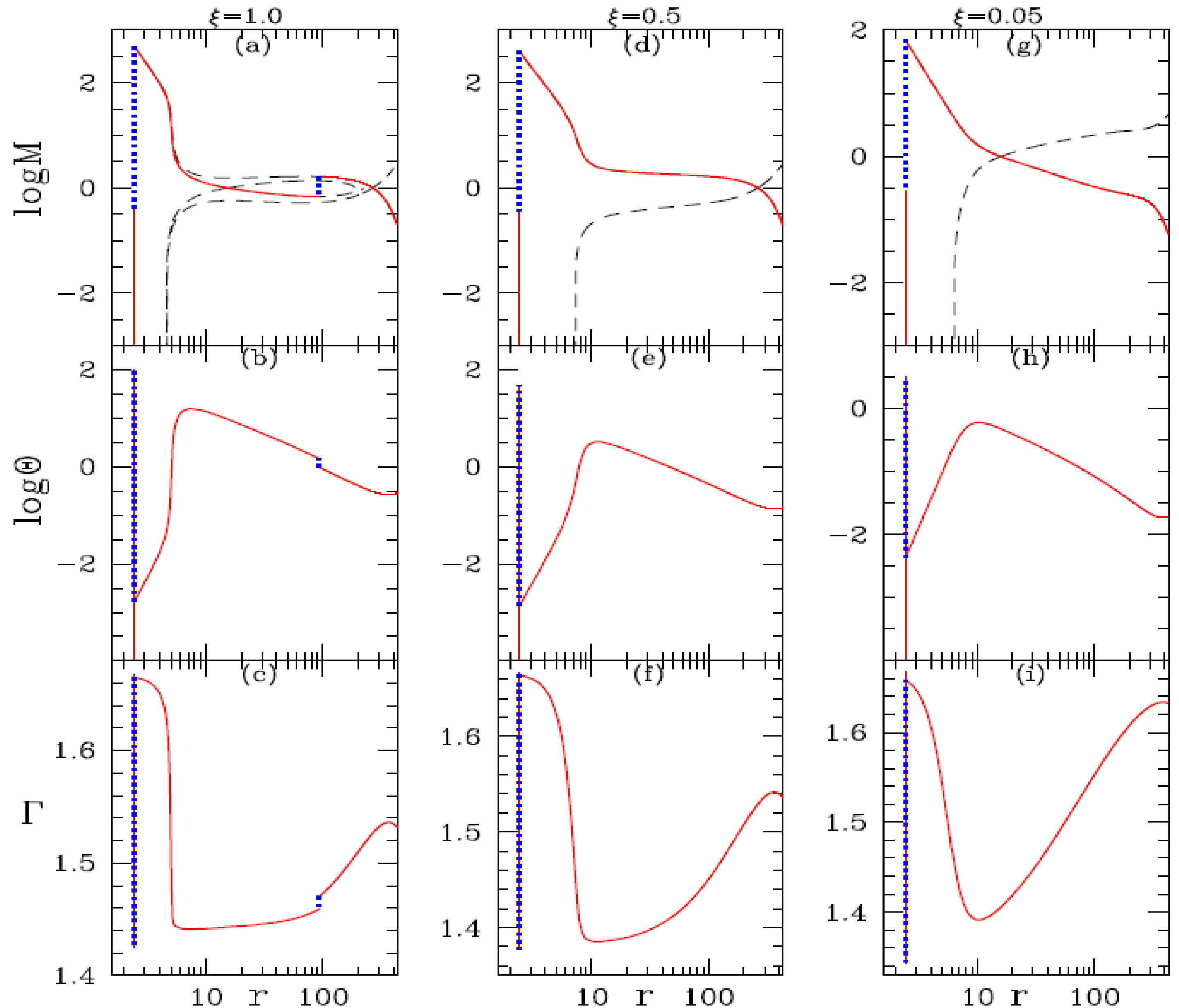

Figure 10. Variation of $\log M$ (a, d, g), $\log \Theta$ (b, e, h), and Γ (c, f, i) as a function of r. Each column of panels represents the flow characterized by $\xi = 1.0$ (a–c), $\xi = 0.5$ (d–f) and $\xi = 0.05$ (g–i). The physical accretion solutions are solid curves with the shock jumps depicted as dotted (blue) vertical lines. The crossing of the dashed and solid curves indicates the position of the sonic points. Here $\dot{M} = 3.51 \times 10^{15}\ \mathrm{g\,s^{-1}}$. The solutions correspond to point ϵ or $\mathcal{B} = 0.998\,77$ and $P = 1\mathrm{s}$ in the $\mathcal{B}$–P parameter space of Fig. 9(a).

Jets launched with same velocity and Mach number

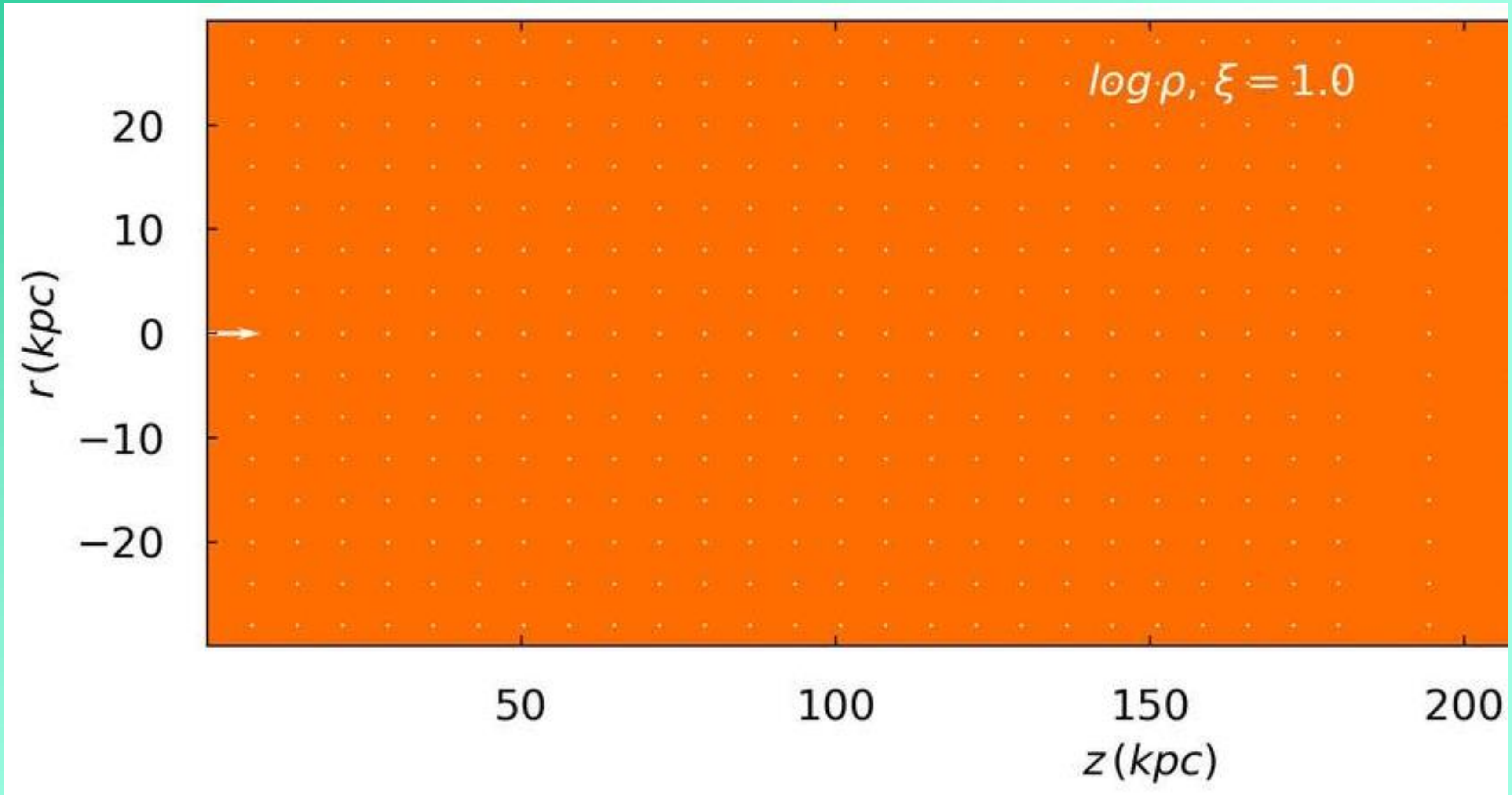

Jets launched with same velocity and Mach number

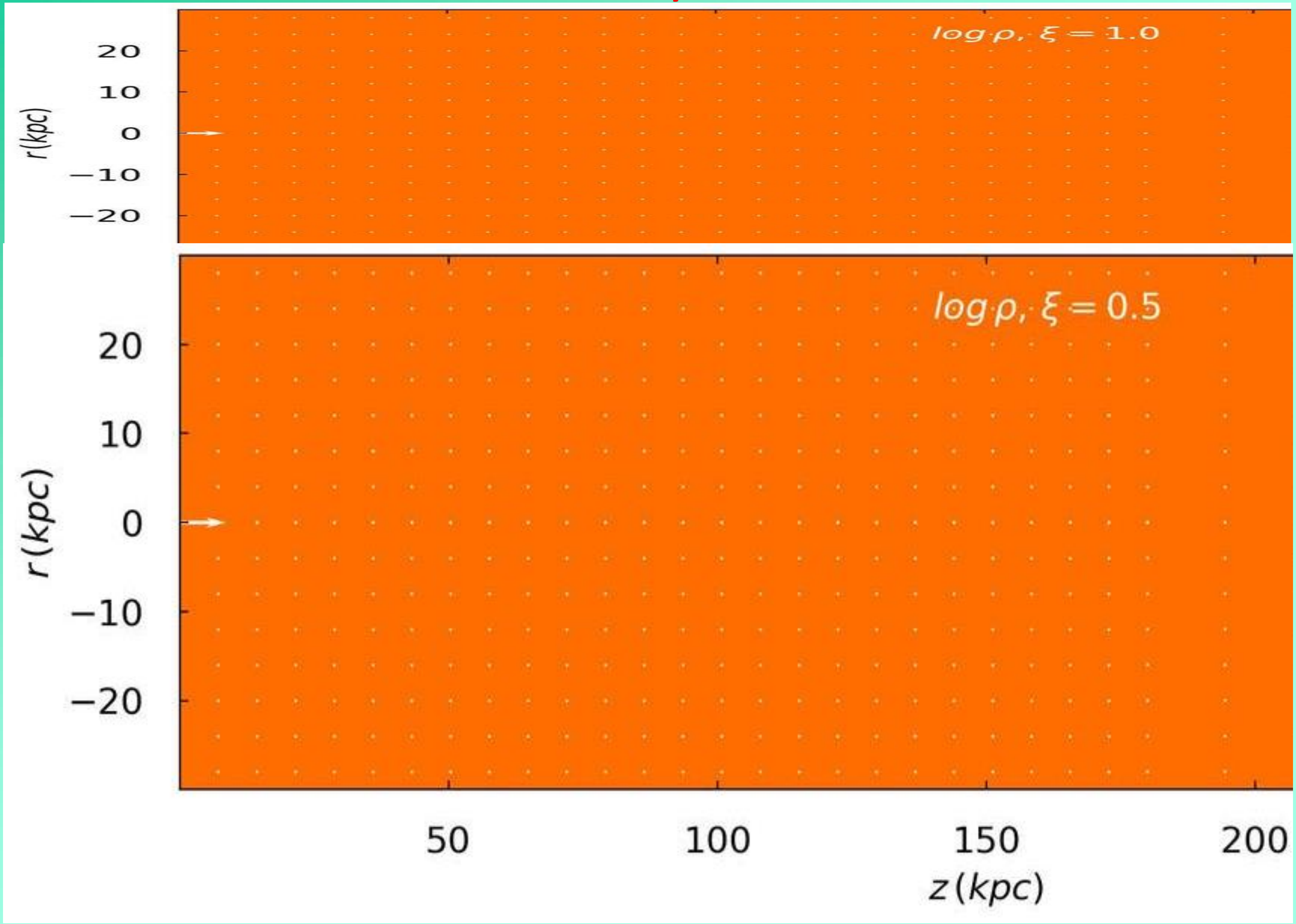

Jet

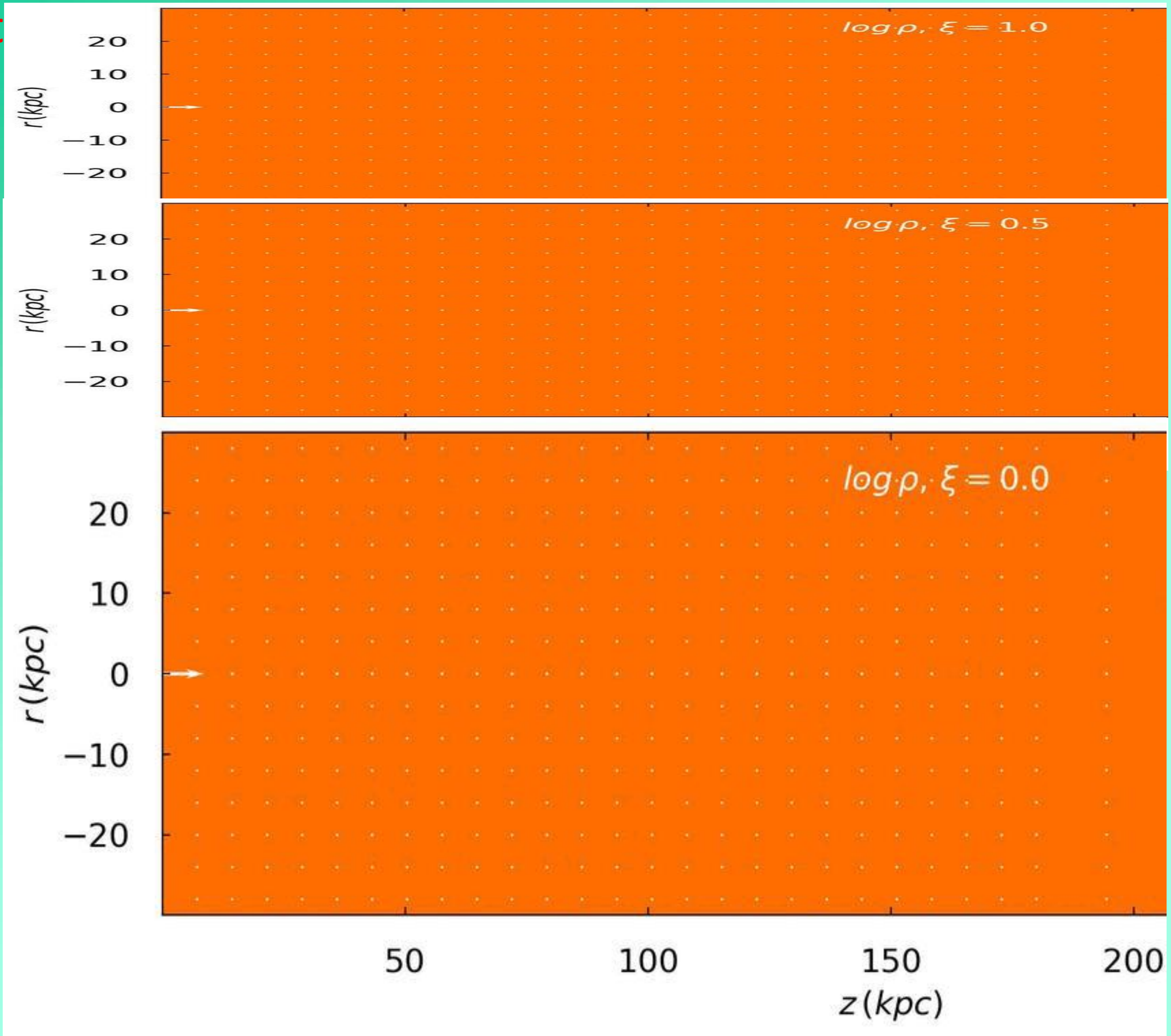

$log\,\rho,\ \xi = 1.0$
$log\,\rho,\ \xi = 0.5$
$log\,\rho,\ \xi = 0.0$
r(kpc)
20
10
0
−10
−20
50
100
150
200
z(kpc)

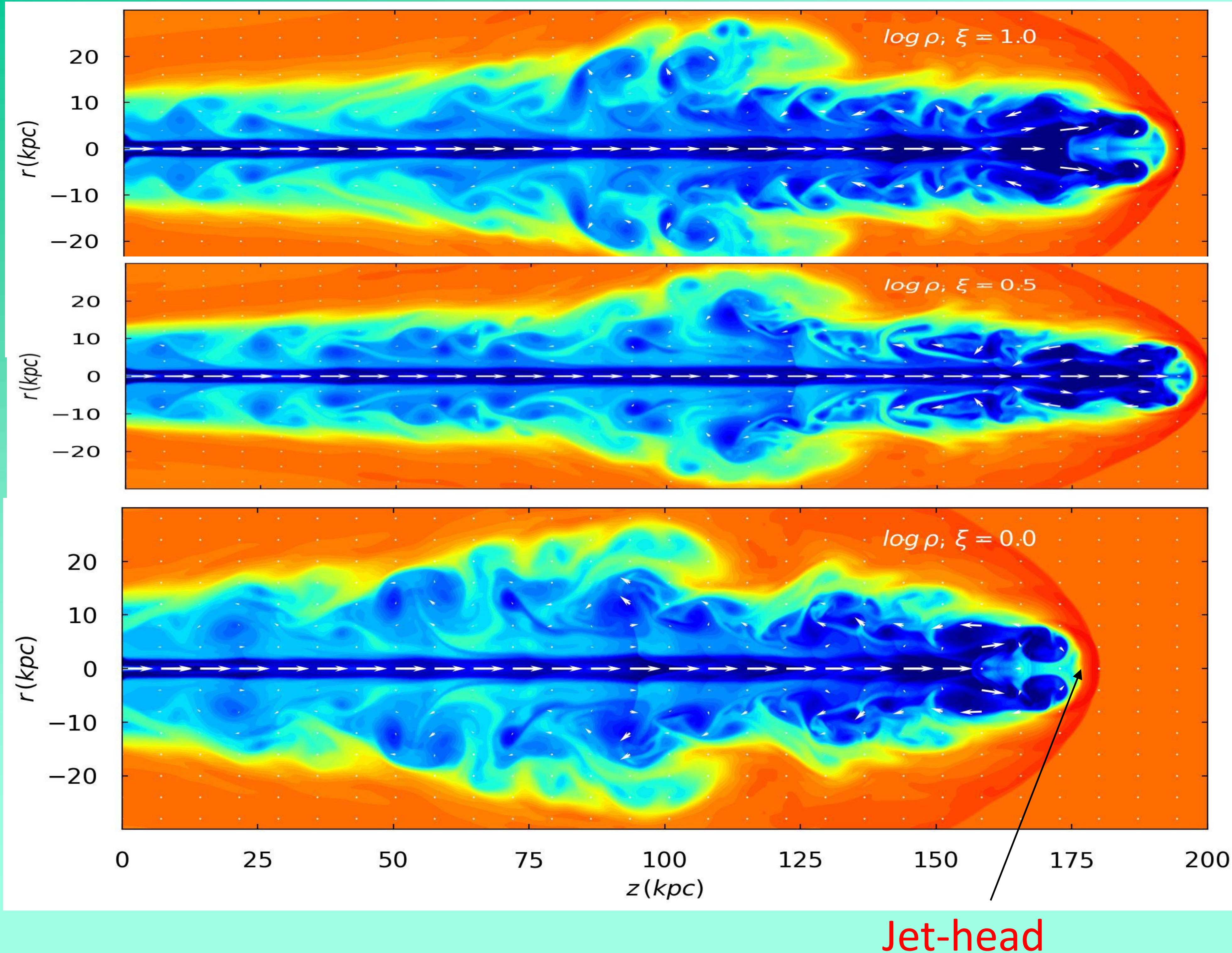

$log\,\rho;\ \xi = 1.0$
$log\,\rho;\ \xi = 0.5$
$log\,\rho;\ \xi = 0.0$
$r\,(kpc)$
$z\,(kpc)$
Jet-head

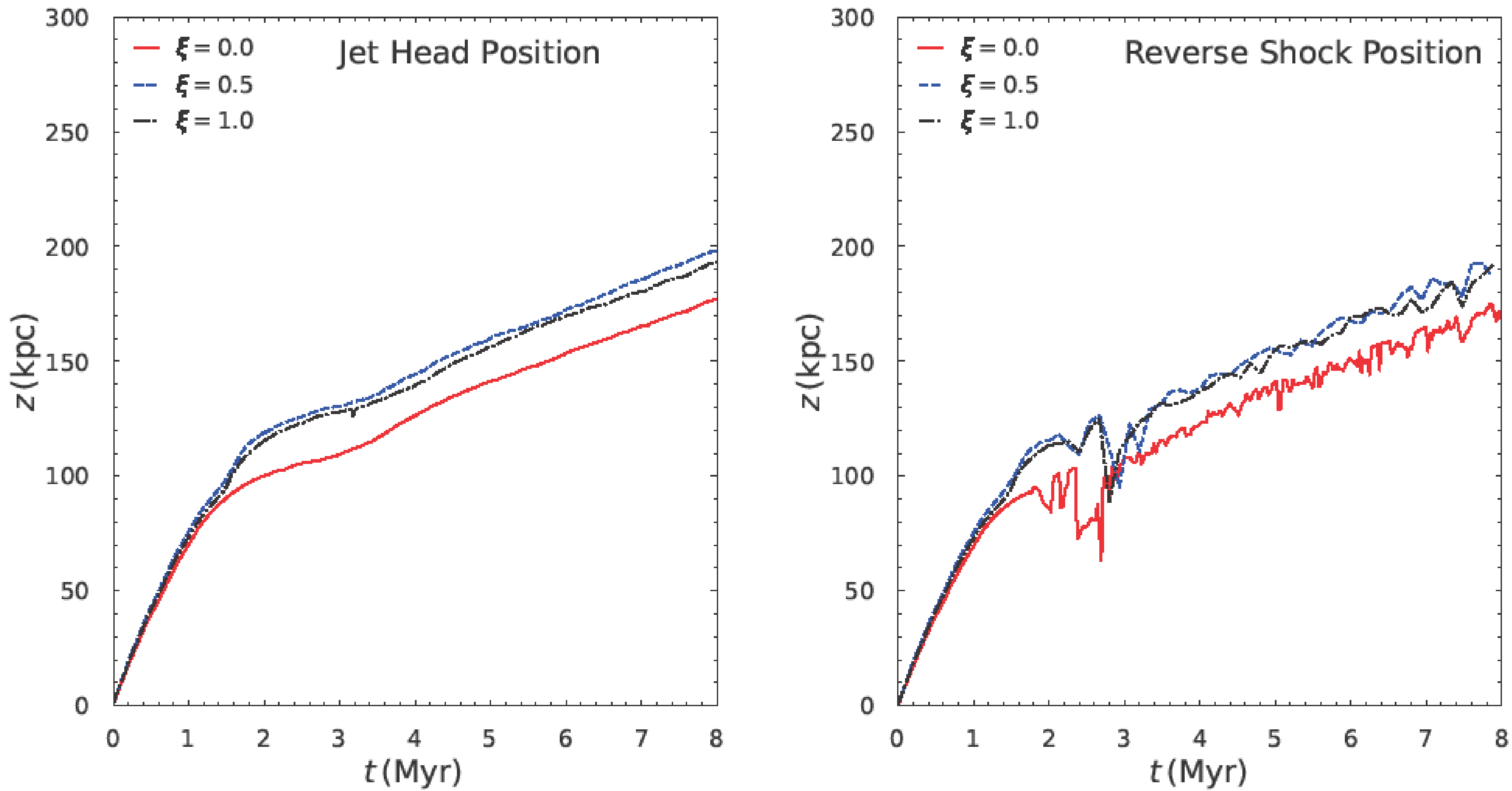
Jet Head Position
Reverse Shock Position
$\xi = 0.0$
$\xi = 0.5$
$\xi = 1.0$
$z\,(\mathrm{kpc})$
$t\,(\mathrm{Myr})$
0
50
100
150
200
250
300
1
2
3
4
5
6
7
8

Same enthalpy jet

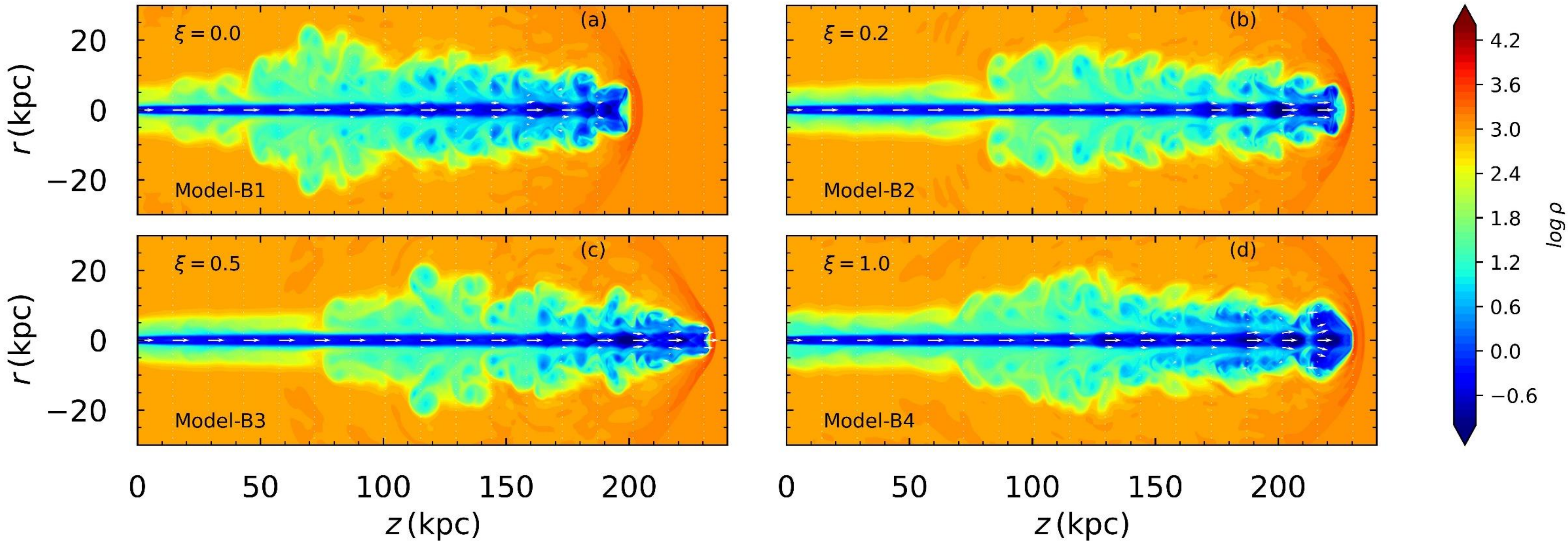

Same enthalpy jet

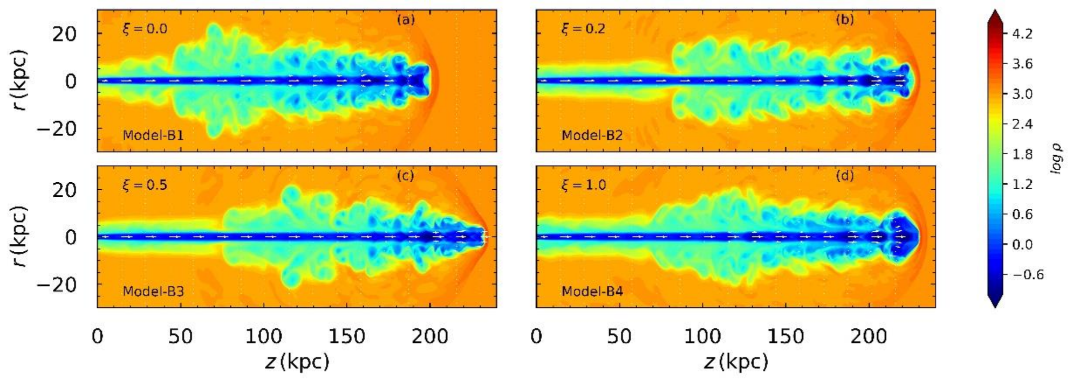

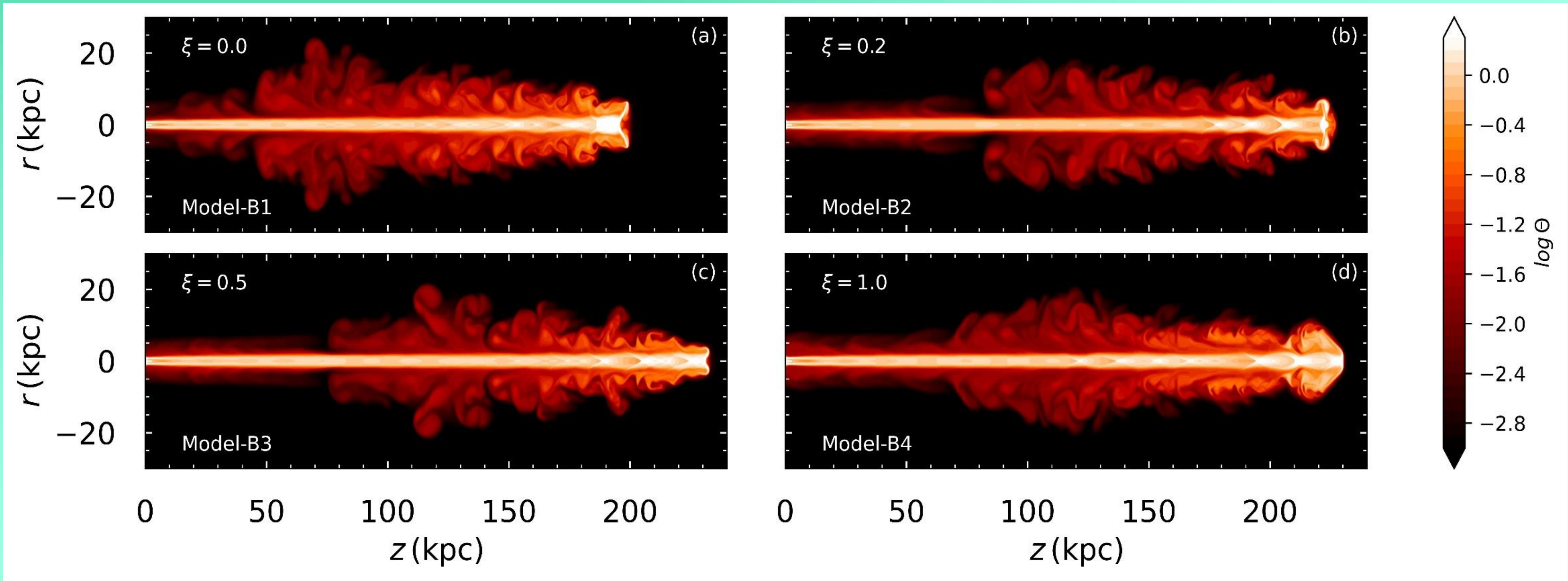

Synchrotron emissivity maps

90º

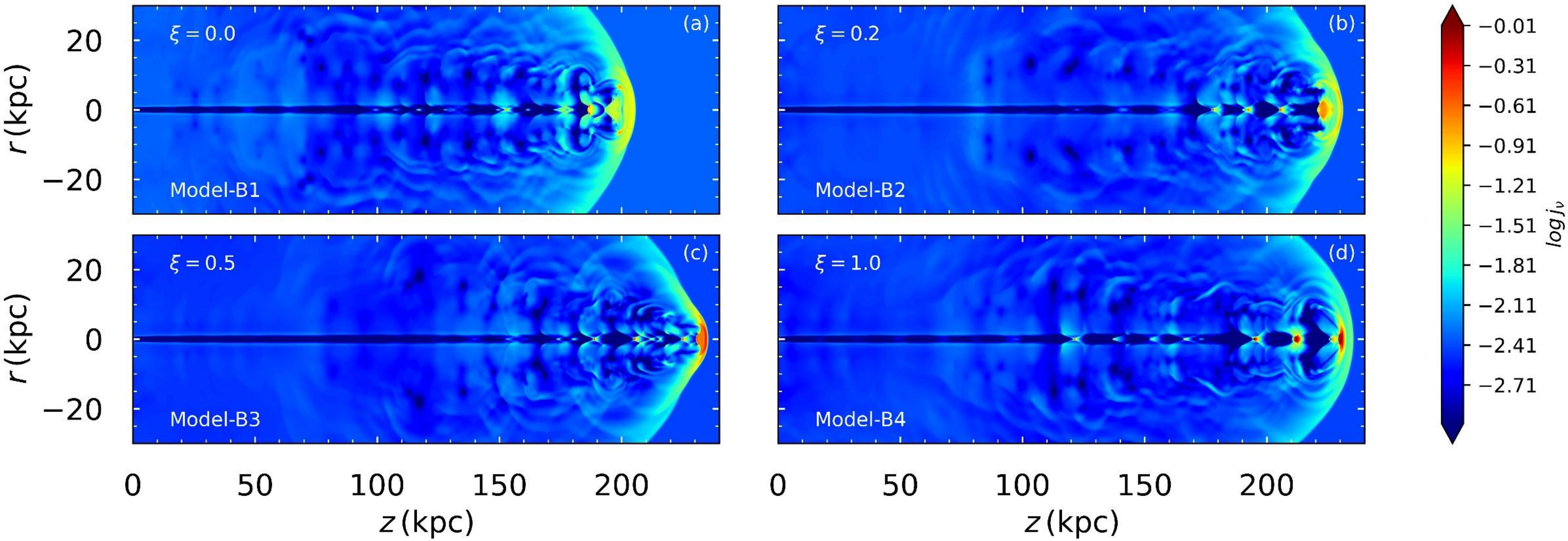

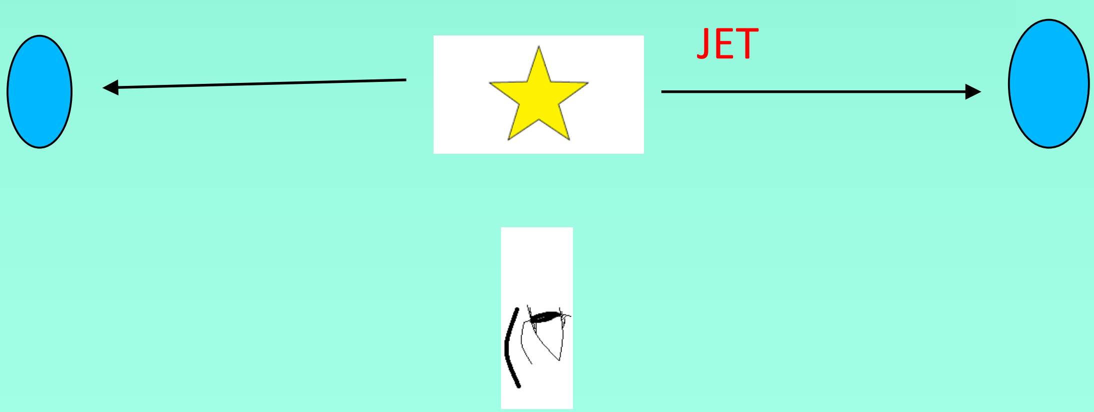

60°

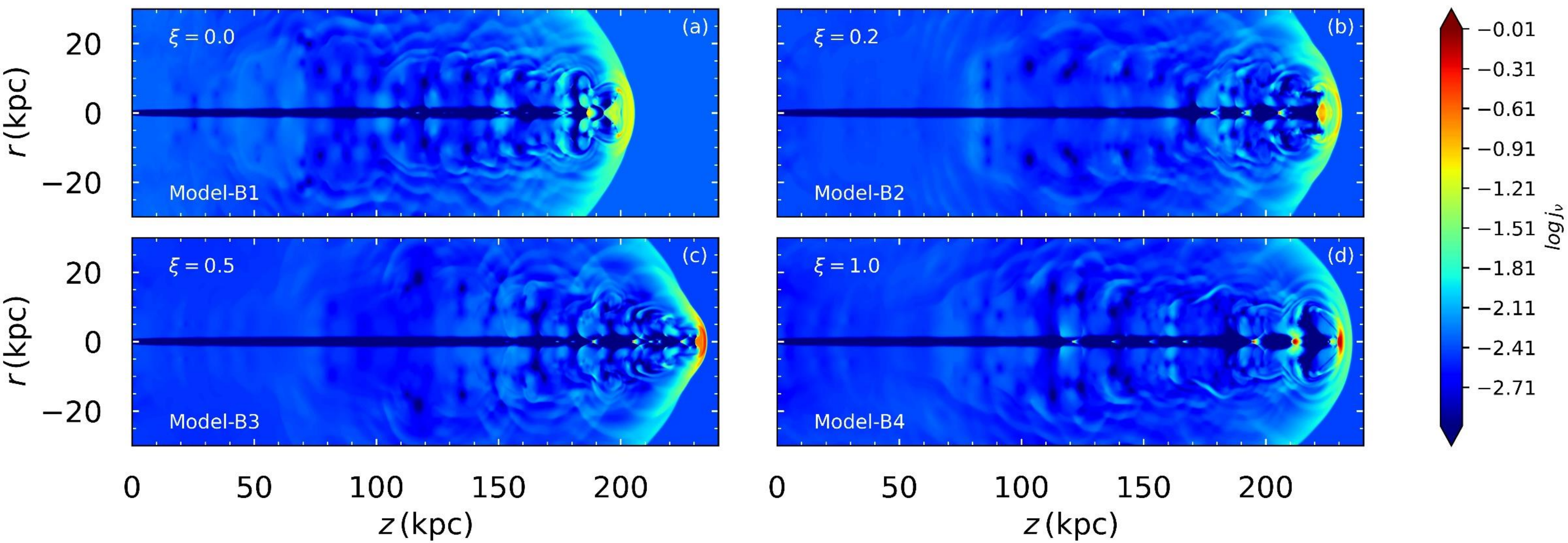

ξ = 0.0
(a)
Model-B1
ξ = 0.2
(b)
Model-B2
ξ = 0.5
(c)
Model-B3
ξ = 1.0
(d)
Model-B4
r (kpc)
z (kpc)
log j_ν
−0.01
−0.31
−0.61
−0.91
−1.21
−1.51
−1.81
−2.11
−2.41
−2.71

45°

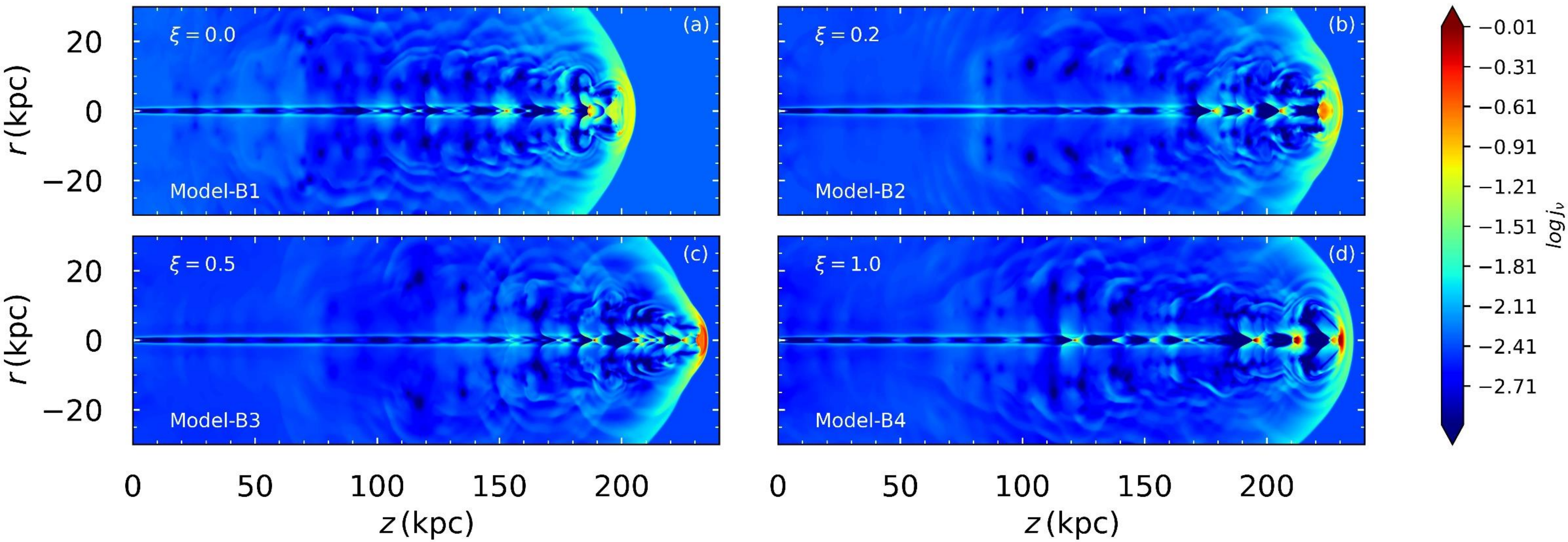

$\xi = 0.0$
(a)
Model-B1
$\xi = 0.2$
(b)
Model-B2
$\xi = 0.5$
(c)
Model-B3
$\xi = 1.0$
(d)
Model-B4
r (kpc)
z (kpc)
20
0
−20
0
50
100
150
200
−0.01
−0.31
−0.61
−0.91
−1.21
−1.51
−1.81
−2.11
−2.41
−2.71
$log\, j_\nu$

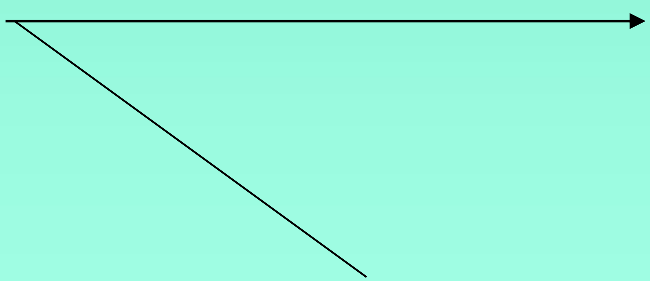

30º

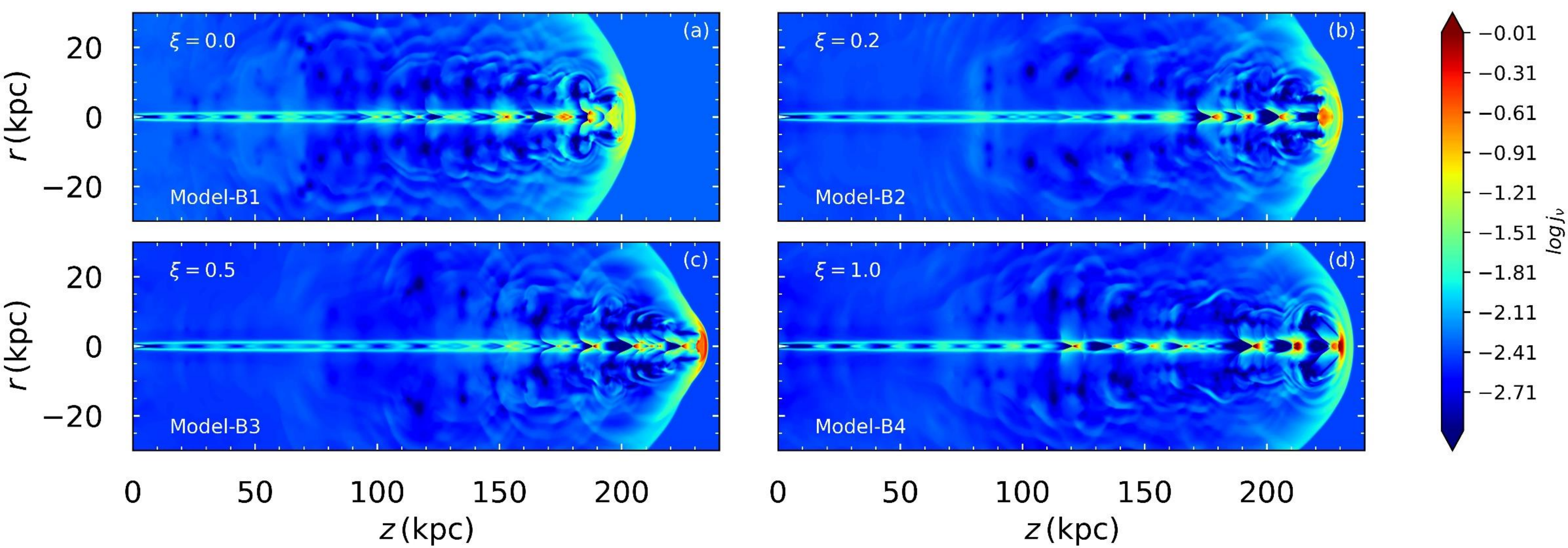

ξ = 0.0
(a)
Model-B1
ξ = 0.2
(b)
Model-B2
ξ = 0.5
(c)
Model-B3
ξ = 1.0
(d)
Model-B4
r (kpc)
z (kpc)
log jν
−0.01
−0.31
−0.61
−0.91
−1.21
−1.51
−1.81
−2.11
−2.41
−2.71

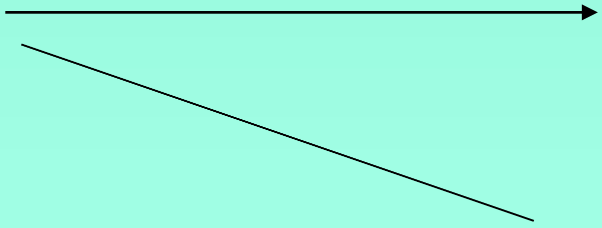

10°

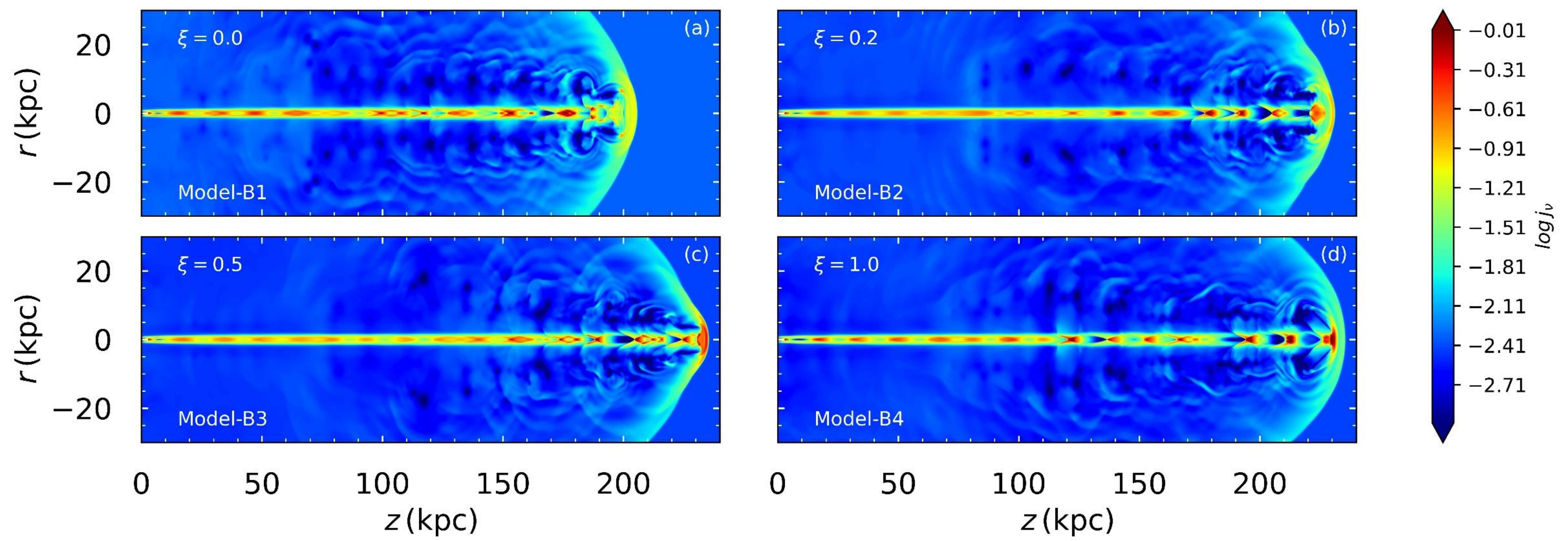

ξ = 0.0
(a)
Model-B1
ξ = 0.2
(b)
Model-B2
ξ = 0.5
(c)
Model-B3
ξ = 1.0
(d)
Model-B4
r (kpc)
20
0
−20
0
50
100
150
200
z (kpc)
−0.01
−0.31
−0.61
−0.91
−1.21
−1.51
−1.81
−2.11
−2.41
−2.71
log jν

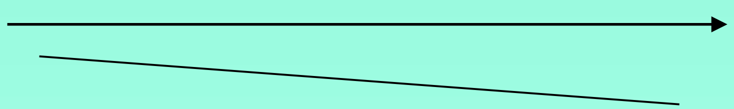

Relativistic MHD Jet

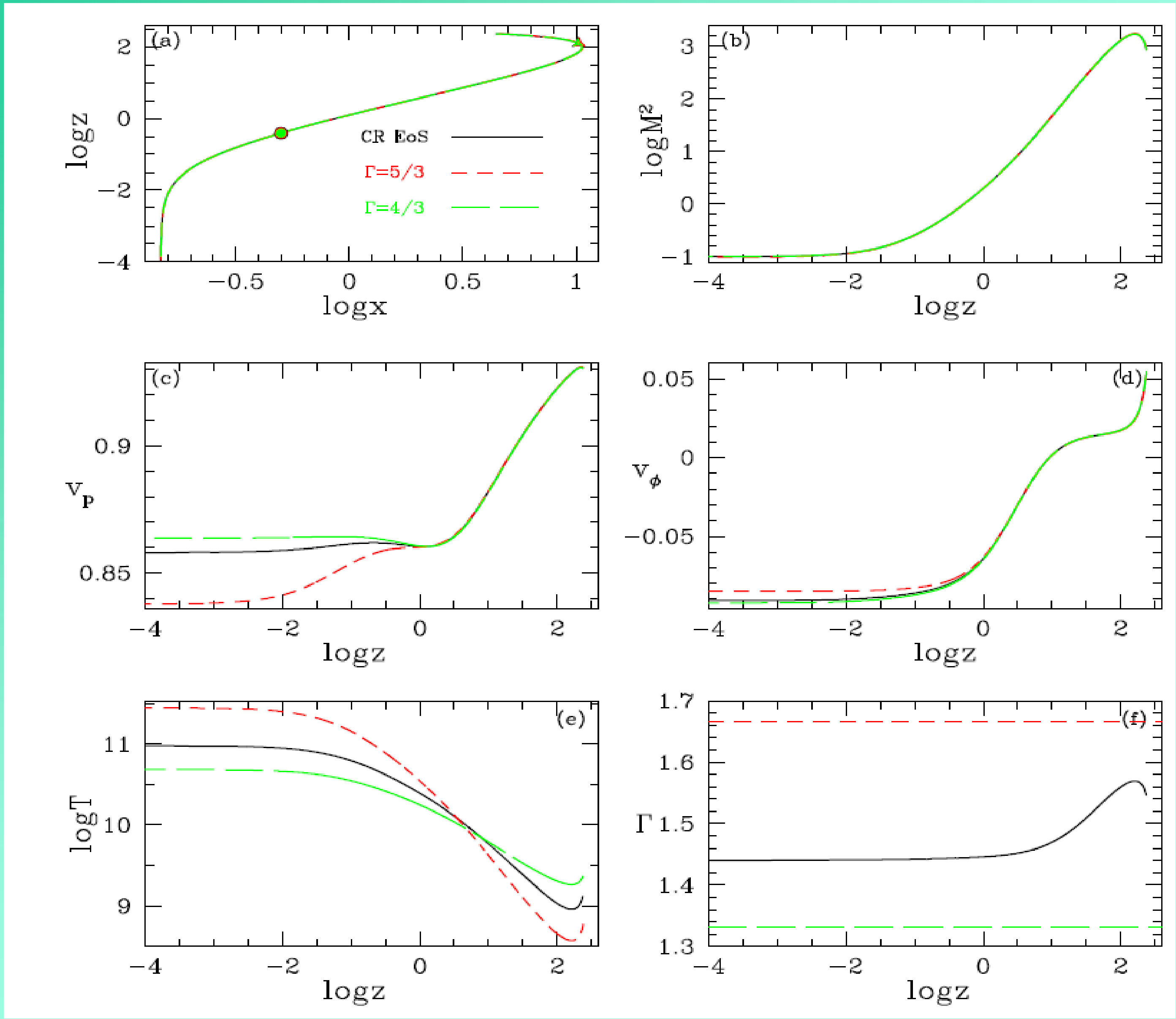

Figure 6. Outflow solutions with variable adiabatic index CR EoS (solid, black) with $\xi = 1$, fixed adiabatic index EoS with $\Gamma = 5/3$ (dashed, red), and $\Gamma = 4/3$ (long dashed, green). All curves are plotted for $\mu = 2.824\ 20$, $x_A^2 = 0.25$, $\theta_A = 52$, $\psi_A = 55$, and $F = 0.8$. Panel (a) Stream line on the xz-plane, (b) $\log M^2$, (c) v_p, (d) v_ϕ, (e) $\log T$, and (f) Γ versus $\log(z)$.

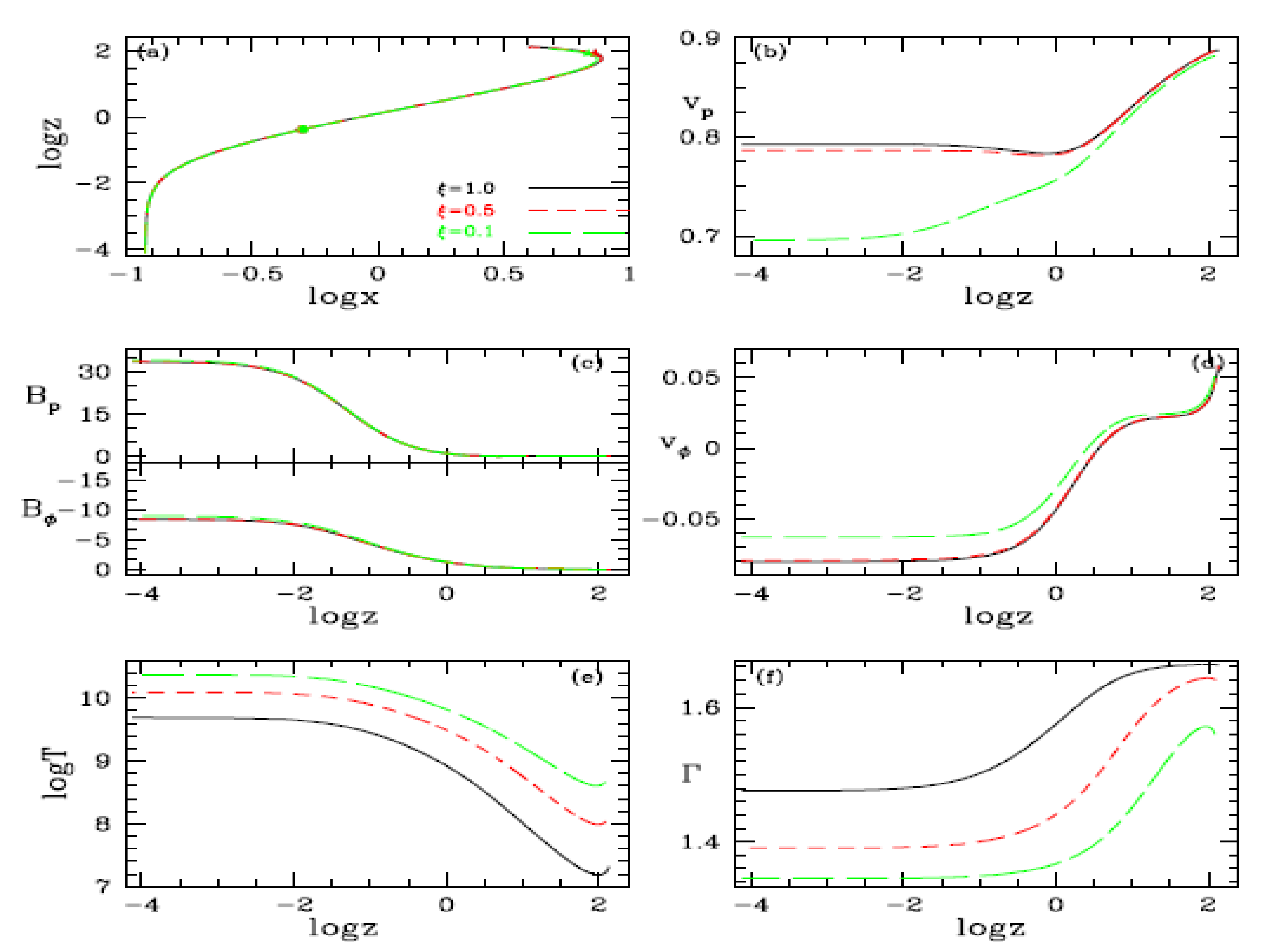

Figure 9. Outflow solutions for different values of $\xi = 1.0$ (solid, black), 0.5 (dashed, red), 0.1 (long-dashed, green). All the curves are plotted for $L = 0.55585$, $\theta_A = 50$, $\psi_A = 55$, $F = 0.75$, and $q = 500$. Panel (a) Stream line on the xz-plane, (b) v_p, (c) B_p and B_ϕ, (d) v_ϕ, (e) $log(T)$, (f) Γ versus $log(z)$.

MhD jet

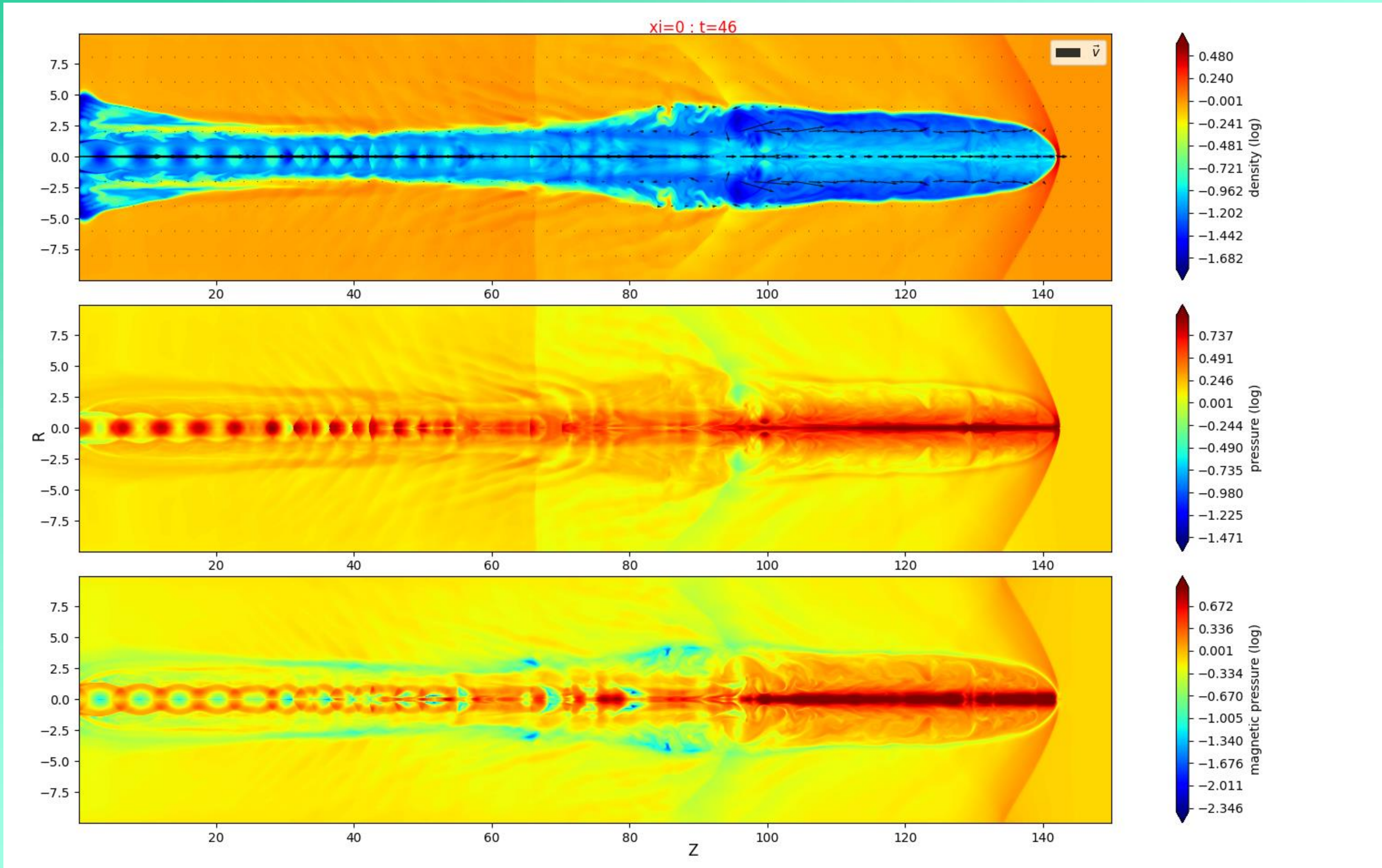
xi=0 : t=46
$\vec{v}$
density (log)
0.480
0.240
−0.001
−0.241
−0.481
−0.721
−0.962
−1.202
−1.442
−1.682
pressure (log)
0.737
0.491
0.246
0.001
−0.244
−0.490
−0.735
−0.980
−1.225
−1.471
magnetic pressure (log)
0.672
0.336
0.001
−0.334
−0.670
−1.005
−1.340
−1.676
−2.011
−2.346
R
Z
7.5
5.0
2.5
0.0
−2.5
−5.0
−7.5
20
40
60
80
100
120
140

MhD jet

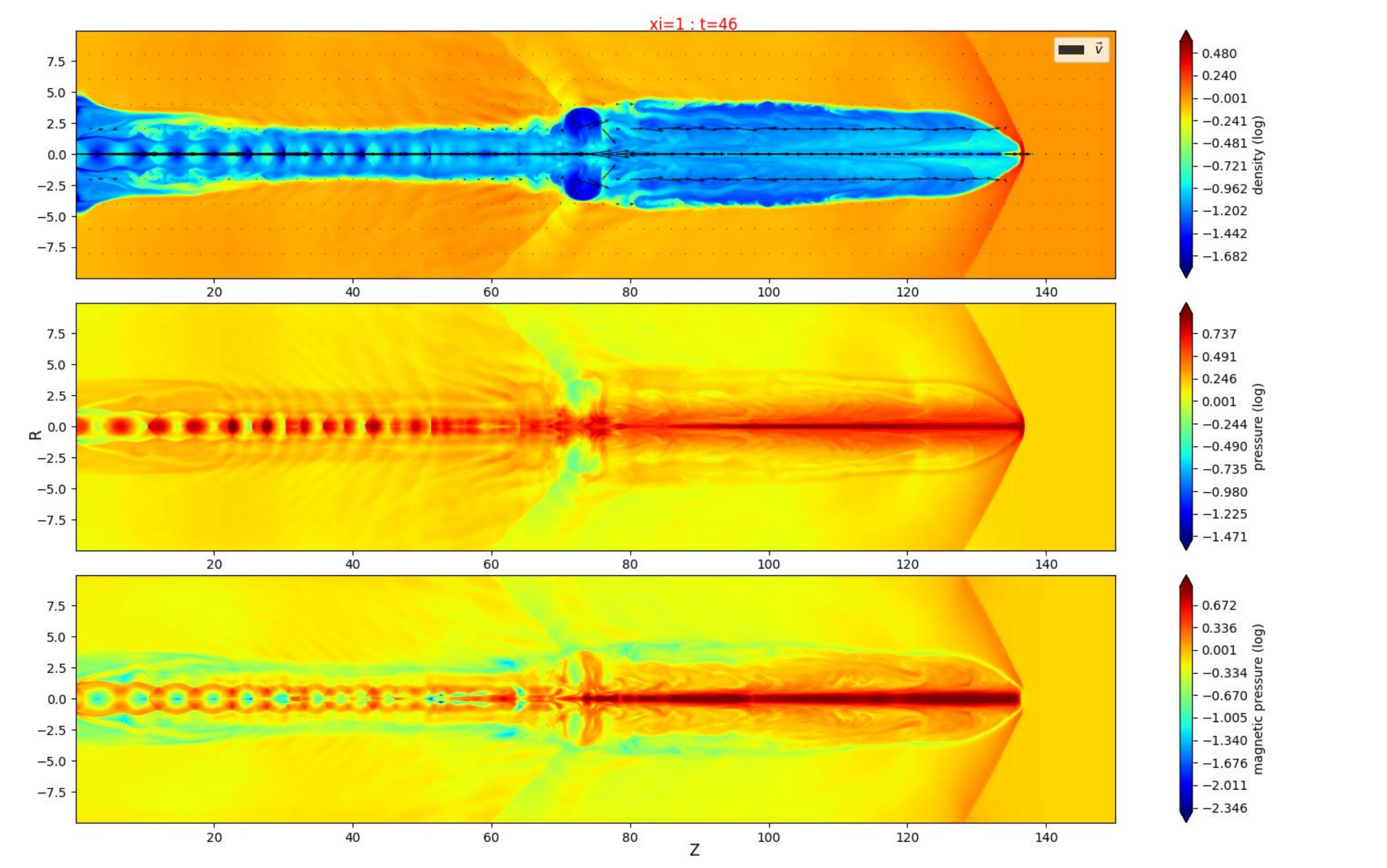

xi=1 : t=46
$\vec{v}$
7.5
5.0
2.5
0.0
−2.5
−5.0
−7.5
20
40
60
80
100
120
140
0.480
0.240
−0.001
−0.241
−0.481
−0.721
−0.962
−1.202
−1.442
−1.682
density (log)
R
0.737
0.491
0.246
0.001
−0.244
−0.490
−0.735
−0.980
−1.225
−1.471
pressure (log)
0.672
0.336
0.001
−0.334
−0.670
−1.005
−1.340
−1.676
−2.011
−2.346
magnetic pressure (log)
Z

Conclusion:

- Composition affects the solution even without considering cooling
- Composition has far greater effect when gravity is present than in the purely special relativistic fluid dynamics, but the effect is also significiant in STR
- It is now important to figure out the observational imprint of composition

Thank you

Historically various disc models

Over the years various models were developed by considering various terms of the equations of motion.

Accretion disc model summary:

$$\frac{\partial(\rho v_r)}{\partial t} + \frac{1}{r}\frac{\partial(r\rho v_r^2)}{\partial r} + \frac{\partial(\rho v_r v_z)}{\partial z} + \frac{\partial P}{\partial r} = -\rho\frac{\partial \Phi}{\partial r} + \frac{\rho l^2}{r^3},$$

(i) **Bondi** – Advective transonic, but <u>no angular momentum</u>, and no dissipation.

Lost favour due to low luminosity

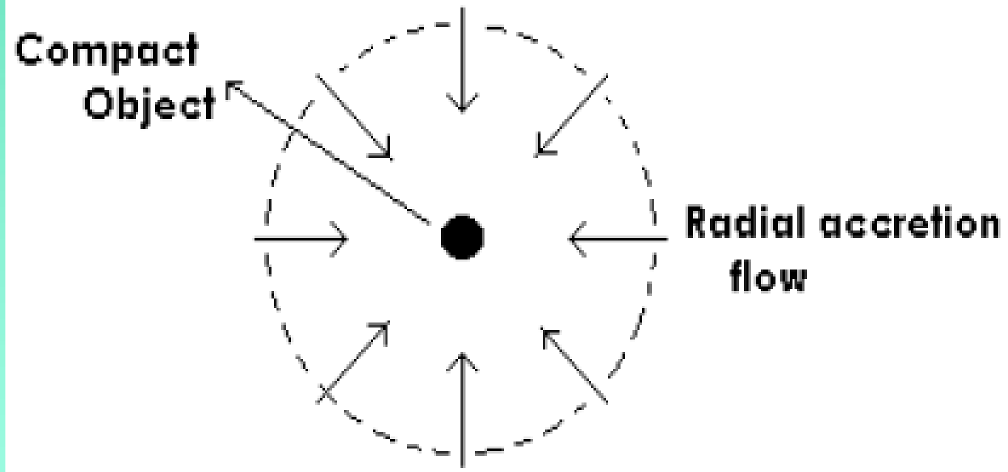

Bondi Accretion

(ii) Keplerian Disc - <u>No advection</u>, <u>no pressure gradient term , cold</u>

(iii) Thick Disc – <u>No advection</u>, hot…

Over the years various models were developed by considering various terms of the equations

Accretion disc model summary:

$$\frac{\partial(\rho v_r)}{\partial t} + \frac{1}{r}\frac{\partial(r\rho v_r^2)}{\partial r} + \frac{\partial(\rho v_r v_z)}{\partial z} + \frac{\partial P}{\partial r} = -\rho\frac{\partial \Phi}{\partial r} + \frac{\rho l^2}{r^3},$$

(i) Bondi – Advective transonic, but no angular momentum, and no dissipation.

(ii) KD - No advection, no pressure gradient term (so thin)

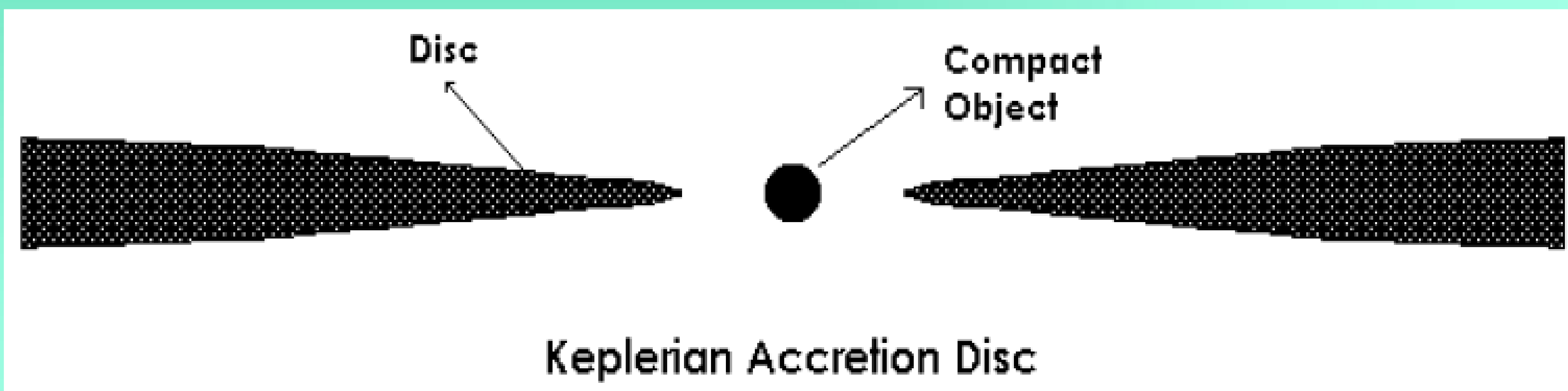

Keplerian Accretion Disc

Luminosity high, but no high energy power law emission.

Over the years various models were developed by considering various terms of the equations

Accretion disc model summary:

$$\frac{\partial(\rho v_r)}{\partial t} + \frac{1}{r}\frac{\partial(r\rho v_r^2)}{\partial r} + \frac{\partial(\rho v_r v_z)}{\partial z} + \frac{\partial P}{\partial r} = -\rho\frac{\partial \Phi}{\partial r} + \frac{\rho l^2}{r^3},$$

(i) Bondi – Advective transonic, but no angular momentum, and no dissipation.

(ii) KD - No advection, no pressure gradient term

(iii) Thick Disc

Unstable.

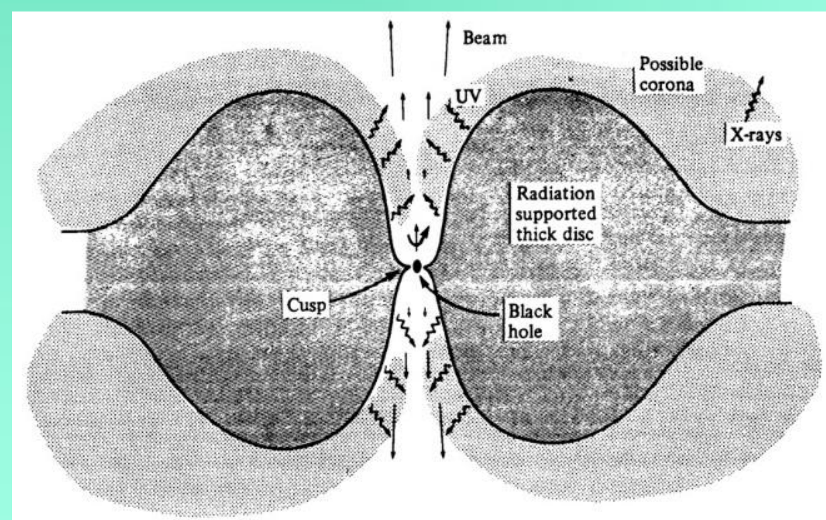

Later Advective discs, ADAF discs… etc

E is the constant of motion and is specified at the horizon. For a given E, different entropy measure (obtained from 1st Law of Therm and conservation of particle flux) corresponds to different solutions.

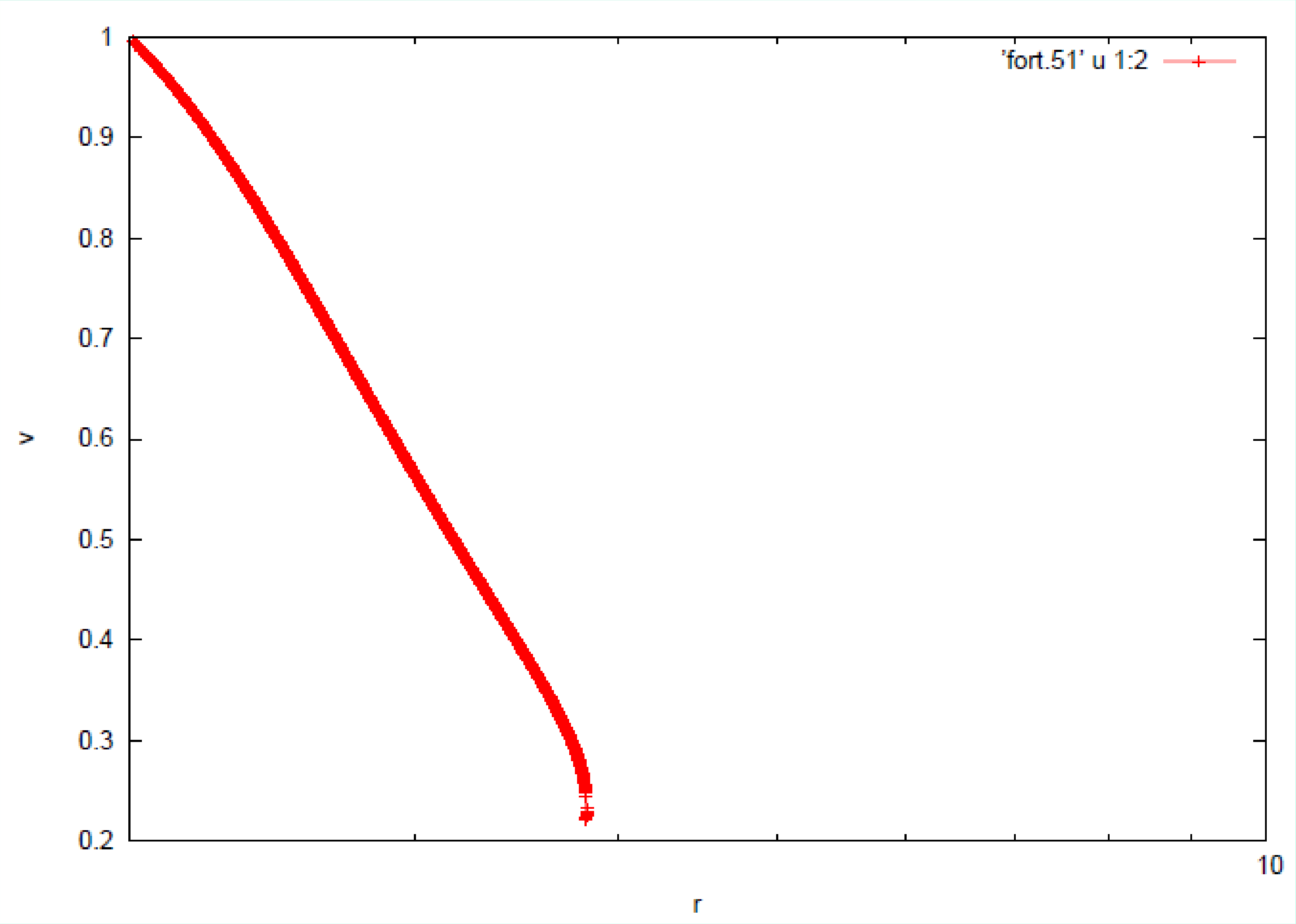

E is the constant of motion and is specified at the horizon. For a given E, different entropy measure (obtained from 1st Law of Therm and conservation of particle flux) corresponds to different solutions.

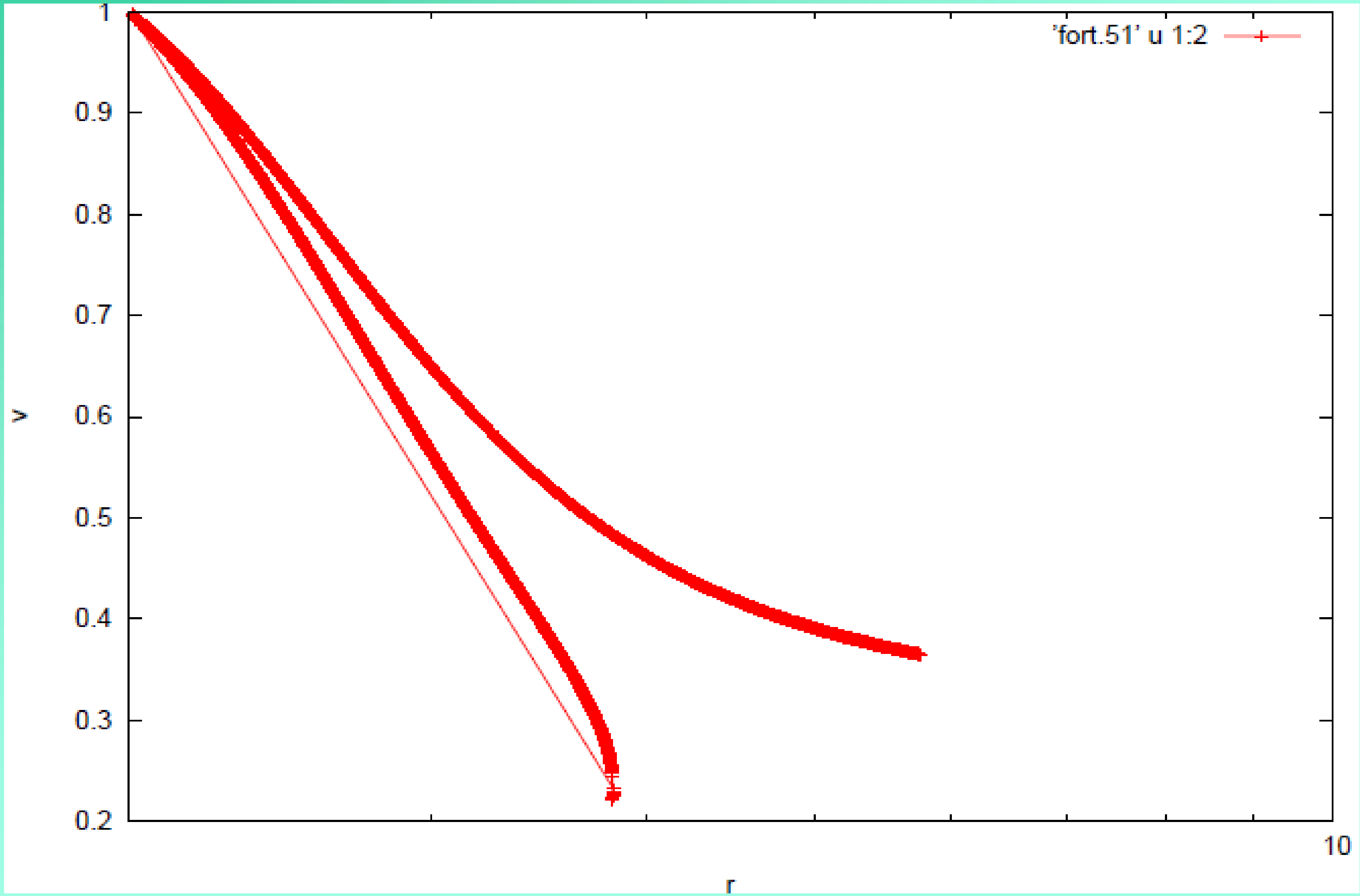

E is the constant of motion and is specified at the horizon. For a given E, different entropy measure (obtained from 1st Law of Therm and conservation of particle flux) corresponds to different solutions.

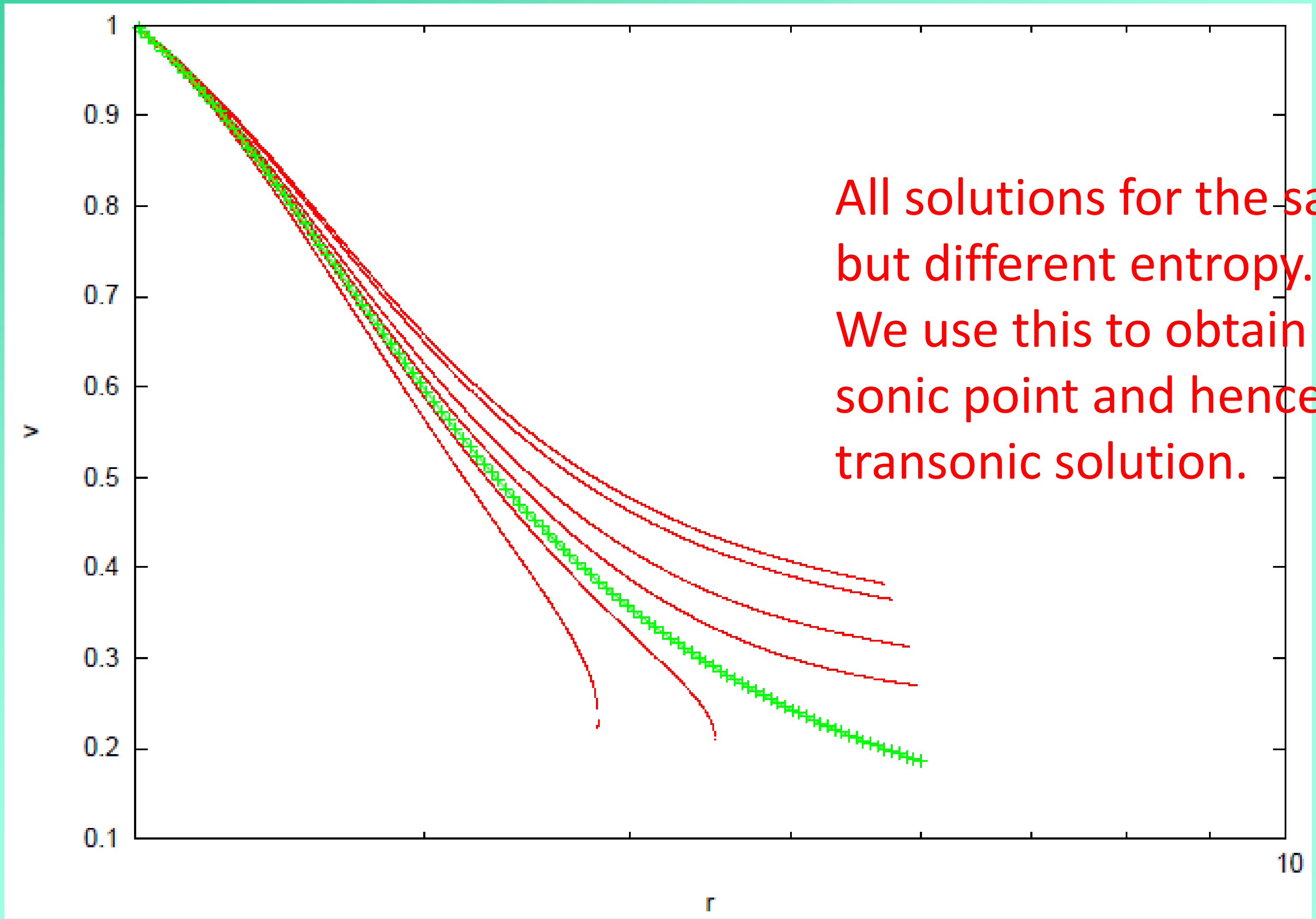

All solutions for the same E but different entropy.
We use this to obtain the sonic point and hence the transonic solution.

Methodology:

Finding a transonic solution without pairs :

- Find sonic points :

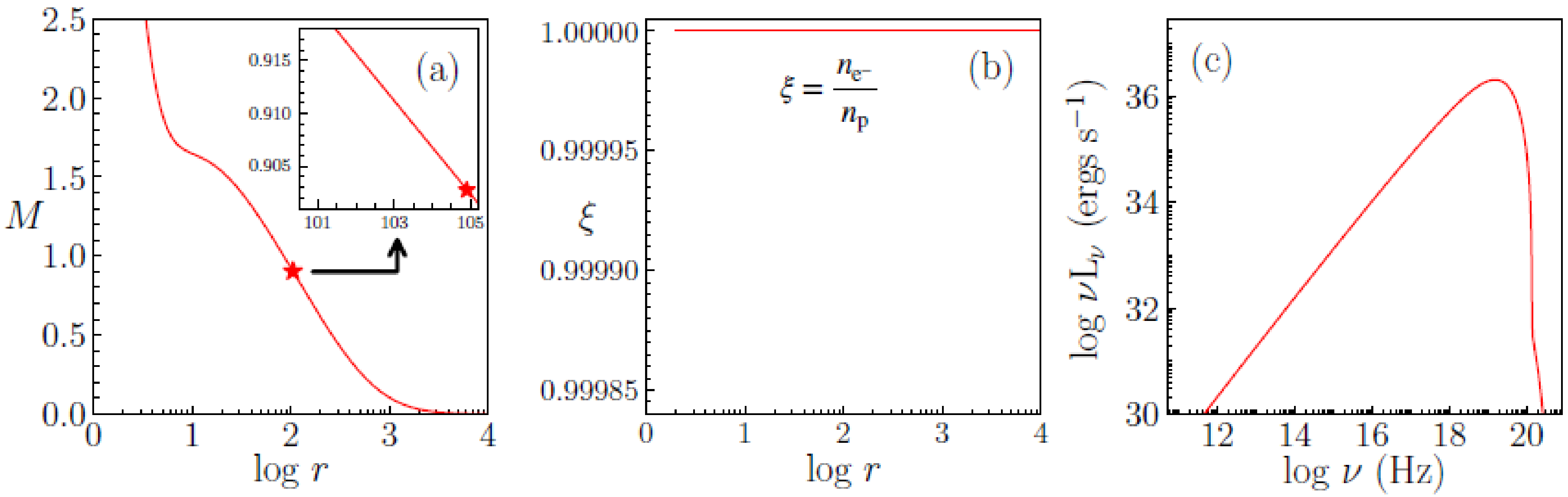

Methodology:

- Finding a transonic solution without pairs :
- Finding a transonic solution with pairs :

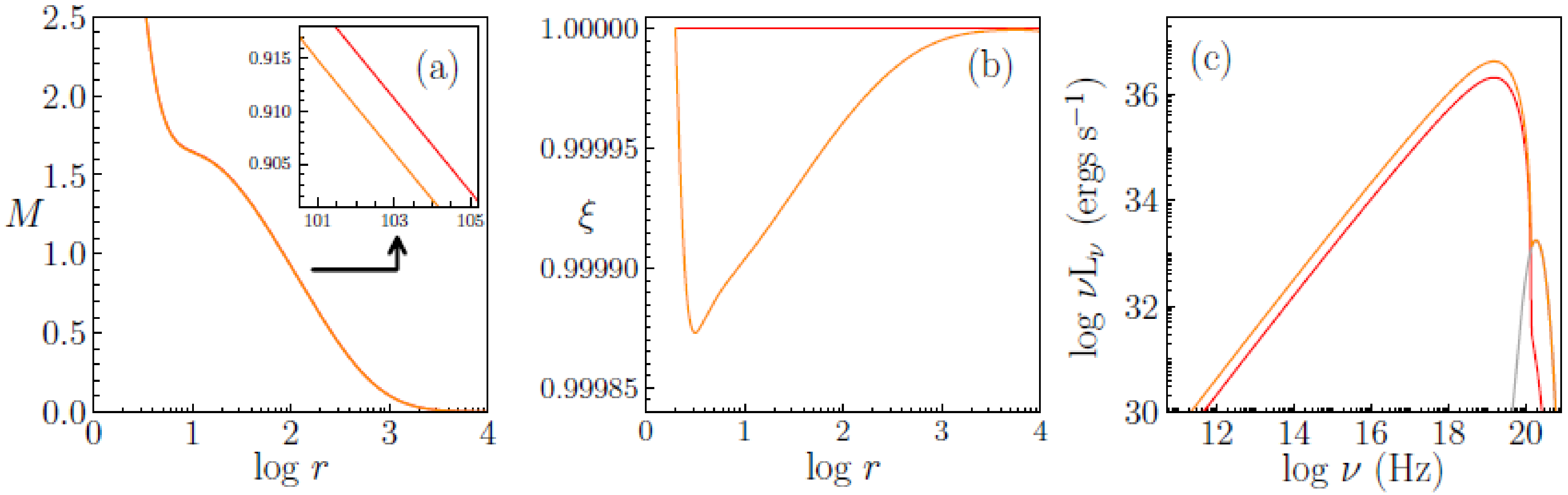

Iteration : 2

Methodology:

- Finding a transonic solution without pairs :
- Finding a transonic solution with pairs :

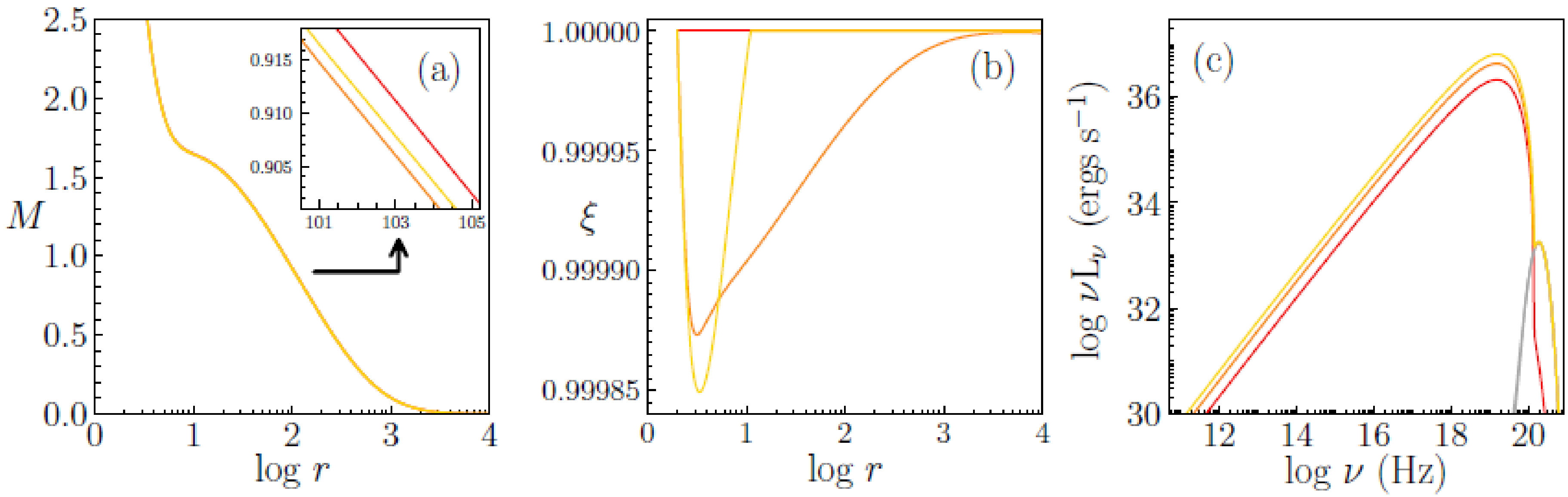

Iteration : 3

Till it converge to a solution.

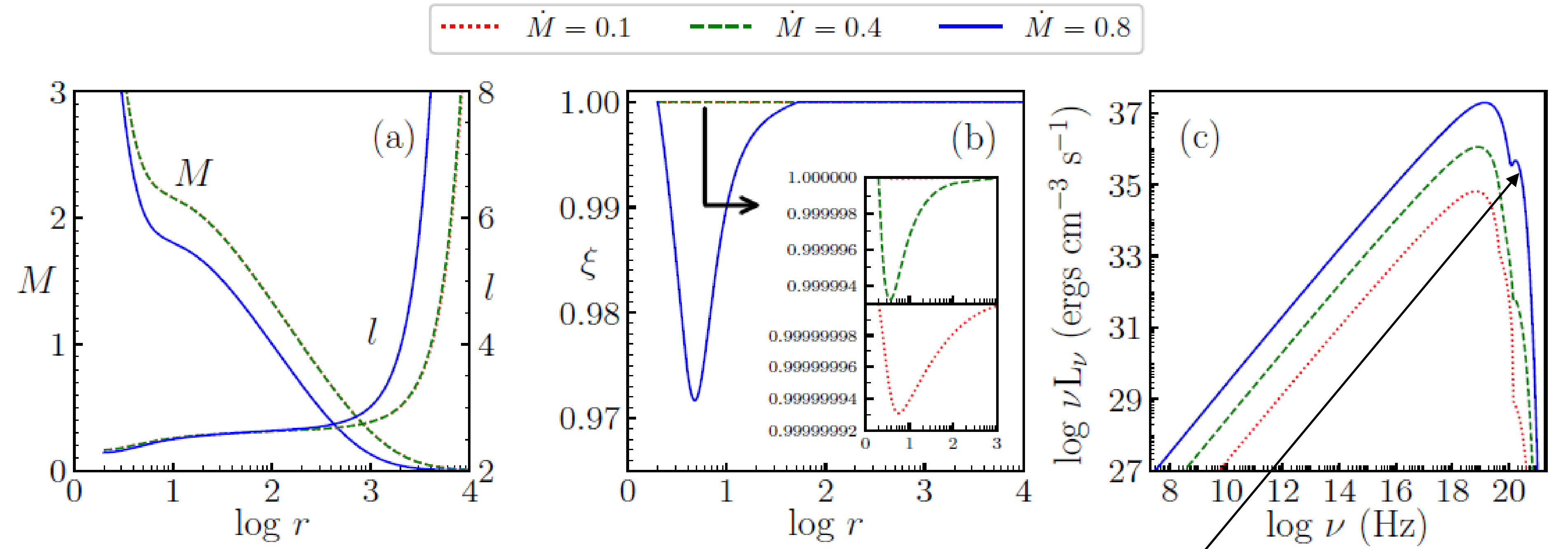

Figure 2: (a) M, l and (b) ξ vs log r plotted for different accretion rates of the system. Their corresponding spectrum is plotted in panel (c). The accretion rates used are: $\dot{M} = 0.1\dot{M}_{\rm edd}$ (red, dotted), $\dot{M} = 0.4\dot{M}_{\rm edd}$ (green, dashed) and $\dot{M} = 0.8\dot{M}_{\rm edd}$ (blue, solid). Rest of the flow parameters are $E = 1.001$, $\lambda_{\rm in} = 2.60$, $\alpha_{\rm v} = 0.01$ and $M_{\rm BH} = 10M_{\odot}$.

For higher accretion rates, pair production is perceptible enough to affect a difference in Mach number M and uφ of the flow and the annihilation line is more pronounced.

Contribution from different parts of the disc

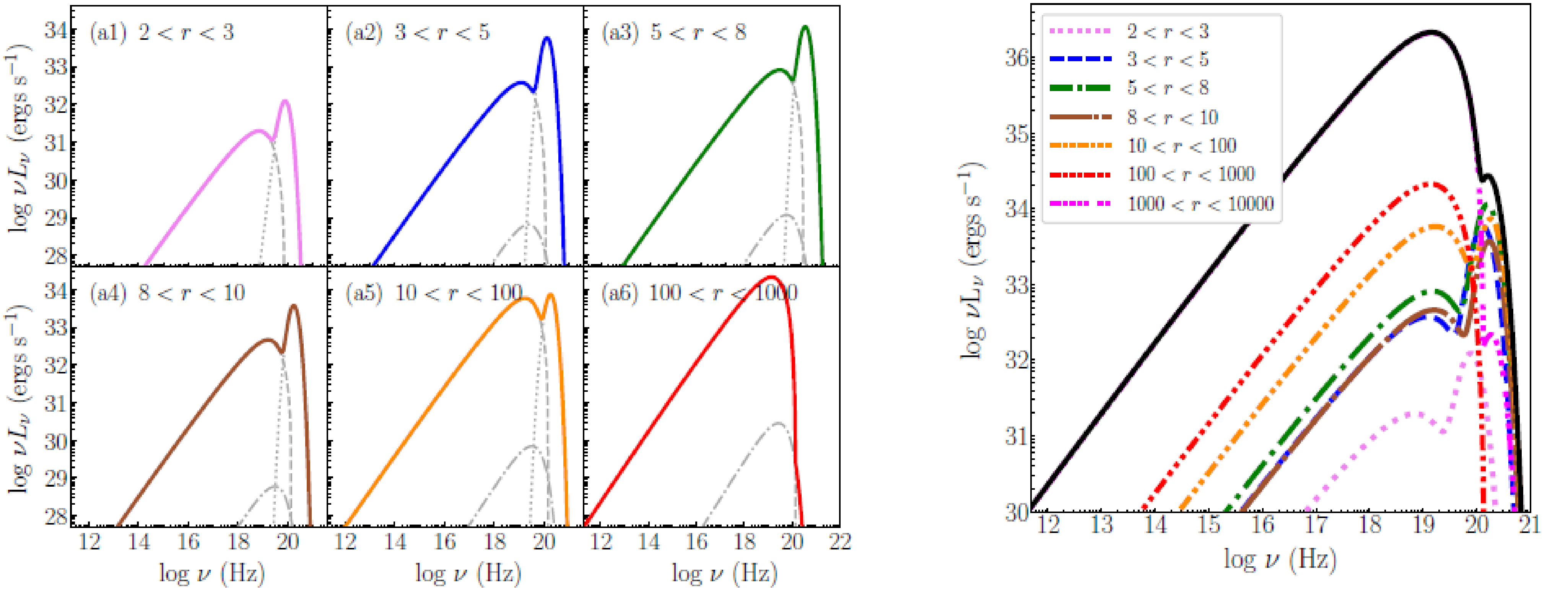

$$E = 1.001,\ \lambda_{\rm in} = 2.70,\ \alpha_{\rm v} = 0.02,\ \dot{M} = 0.8\dot{M}_{\rm edd},\ M_{\rm BH} = 10M_{\odot}$$